ESI: Barium phosphidoboranes and related calcium complexes

Gabriel Duneș,[†] Peter. M. Chapple,[†] Samia Kahlal, Thierry Roisnel,
Jean-François Carpentier, Jean-Yves Saillard* and Yann Sarazin*

Univ Rennes, CNRS, ISCR-UMR 6226, 35000 Rennes, France.

* Corresponding authors. E-mail address:
jean-yves.saillard@univ-rennes.fr
yann.sarazin@univ-rennes.fr

[†] These two co-authors have contributed equally to the work, and must both be considered as first co-author.

Table of Contents

EXPERIMENTAL SECTION

General procedures. All manipulations were performed under an inert atmosphere by using standard Schlenk techniques or in a dry, solvent-free glovebox (Jacomex; O_2 < 1 ppm, H_2O < 3 ppm). Thf was distilled under argon from Na/benzophenone prior to use. Thp was dried over KOH, then was distilled over K/benzophenone prior to use. Petroleum ether (45-65 °C), toluene, dichloromethane, and Et_2O were collected from MBraun SPS-800 purification alumina columns and thoroughly degassed with argon before being stored on 4 Å molecular sieves. Deuterated solvents (Eurisotop, Saclay, France) were stored in sealed ampoules over activated 4 Å molecular sieves or a potassium mirror, and degassed by a minimum of three freeze–thaw cycles. NMR spectra were recorded with Bruker AM-400 or AM-500 spectrometers. All chemical shifts (δ) [ppm] were determined relative to the residual signal of the deuterated solvent or to an external standard in benzene-d_6 or toluene-d_8. Assignment of the signals was assisted by 1D (^{1}H, ^{13}C) and 2D (COSY, HMBC, HMQC, NOE) NMR experiments. Reliable and reproducible elemental analysis could not be obtained for the metal complexes, most probably due to their very high moisture-sensitivity. The proligand {Carb}H[1] and the precursors [{Carb}BaN(SiMe$_3$)$_2$],[1] [{Carb}CaN(SiMe$_3$)$_2$][1] and HPPh$_2$.B(C$_6$F$_5$)$_3$[2] were prepared following literature methods. The precursors [Ae{N(SiMe$_3$)$_2$}$_2$] and [Ae{N(SiMe$_3$)$_2$}$_2$.(thf)$_2$] were obtained upon modification of Boncella's metathetical protocol, using CaI_2 or BaI_2 and KN(SiMe$_3$)$_2$ as starting materials.[3] HPPh$_2$.BH$_3$ was prepared upon reaction of HPPh$_2$ and BH$_3$.SMe$_2$ by adaptation of a known procedure.[4] All other chemicals were provided by regular commercial suppliers and used as received.

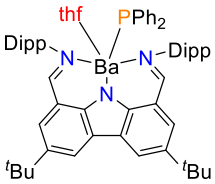

[{Carb}BaPPh$_2$.(thf)] (1.(thf)). Neat HPPh$_2$ (5.1 µL, 29.3 µmol) was added with a microsyringe to a J-Young's tube containing [{Carb}BaN(SiMe$_3$)$_2$.(thf)] (30 mg, 29.3 µmol) in deuterated toluene (0.6 mL). The NMR tube was sealed, briefly shaken and run immediately on an NMR spectrometer.

^{1}H NMR (400.16 MHz, 298 K, toluene-d_8): δ 8.63 (br s, 2H, C*H*-Carb), 8.36 (s, 2H, C*H*=N), 7.59 (br s, 2H, C*H*-Carb), 7.24 (br, 4H, *o*-C$_6$*H*$_5$), 7.07-6.97 (m, 6H, C$_6$*H*$_3$-Dipp), 6.47 (t, $^3J_{HH}$ = 7.5, 4H, *m*-C$_6$*H*$_5$), 6.24 (t, $^3J_{H\text{-}H}$ = 6.5, 2H, *p*-C$_6$*H*$_5$), 3.03 (hept, $^3J_{H\text{-}H}$ = 6.0, 4H, C*H*(CH$_3$)$_2$), 2.77 (m, 4H, OC*H*$_2$) 1.50 (s, 18H, C(C*H*$_3$)$_3$), 1.14 (d, $^3J_{H\text{-}H}$ = 6.6, 12H, CH(C*H*$_3$)$_2$), 1.10 (m, 4H, OCH$_2$C*H*$_2$), 1.02 (d, $^3J_{H\text{-}H}$ = 6.8, 12H, CH(C*H*$_3$)$_2$) ppm.

^{31}P NMR{^{1}H} (161.99 MHz, 298 K, toluene-d_8): δ 3.2 (br s) ppm.

^{13}C NMR data could not be recorded as the title compound decomposes rapidly during collection to a range of products, including the reductive coupling product Ph$_2$P–PPh$_2$ detected by ^{31}P NMR.

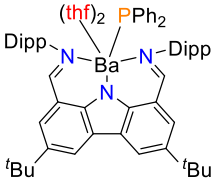

[{Carb}BaPPh$_2$.(thf)$_2$] (1.(thf)$_2$). Neat HPPh$_2$ (60 mg, 0.33 mmol) was added dropwise to a solution of [{Carb}BaN(SiMe$_3$)$_2$] (300 mg, 0.32 mmol) in petroleum ether (30 mL) at –78 °C, resulting in an instant colour change from yellow to blood orange. The reaction was warmed up to room temperature over 1 h, during which

time a bright orange solid precipitated out of solution. The solid was isolated by cannula filtration, washed with petroleum ether (3×20 mL) and recrystallised from a petroleum ether/thf solution at –30 °C to give the title compound in about 10-15 mg isolated yield of single crystals. If the crude solution is instead taken to dryness, the ^{1}H NMR and ^{31}P NMR data are unclear but indicate a mixture of (at least) two major products.

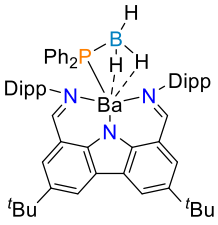

[{Carb}Ba(PPh$_2$.BH$_3$)] (2). In Schlenk flask, [{Carb}BaN(SiMe$_3$)$_2$] (300 mg, 0.32 mmol) and HPPh$_2$.BH$_3$ (64 mg, 0.32 mmol) were dissolved in petroleum ether (30 mL), generating a yellow solution. Stirring at room temperature for 1 h. Evacuation of the volatiles then gave the desired product as a yellow solid. Yield: 297 mg (94%). Despite repeated attempts, this compound could not be recrystallised.

^{1}H NMR (500.1 MHz, 300 K, benzene-d_6,): δ 8.60 (d, $^{4}J_{H\text{-}H}$ = 2.1, 2H, C*H*-Carb), 8.36 (s, 2H, C*H*=N), 7.59 (d, $^{4}J_{H\text{-}H}$ = 2.1, 2H, C*H*-Carb), 7.20 (br, 4H, C$_6$*H*$_5$), 7.17-7.13 (m, 6H, C$_6$*H*$_3$-Dipp), 6.92 (br, 6H, C$_6$*H*$_5$), 3.08 (hept, $^{3}J_{H\text{-}H}$ = 6.5, 4H, C*H*(CH$_3$)$_2$), 1.46 (s, 18H, C(C*H*$_3$)$_3$), 1.26 (d, $^{3}J_{H\text{-}H}$ = 6.9, 12H, CH(C*H*$_3$)$_2$), 1.03 (d, $^{3}J_{H\text{-}H}$ = 6.7, 12H, CH(CH$_3$)$_2$) ppm. The resonances for boron-bound H atoms could not be detected.

^{13}C{^{1}H} NMR (125.8 MHz, 298 K, benzene-d_6): δ 172.16 (*C*H=N), 149.41 (Ar-*C*), 148.21 (Ar-*C*), 140.45 (Ar-*C*), 138.66 (Ar-*C*), 133.93 (br, *o*-*C*$_6$H$_5$), 133.80 (br, *m*-*C*$_6$H$_5$),132.39 (Ar-*C*), 126.59 (br, *p*-*C*$_6$H$_5$), 125.95 (Ar-*C*), 124.45 (Ar-*C*), 123.88 (Ar-*C*), 122.77 (Ar-*C*), 119.76 (Ar-*C*), 34.45 (*C*(CH$_3$)$_3$), 32.18 (C(*C*H$_3$)$_3$), 29.18 (*C*H(CH$_3$)$_2$), 25.54 (CH(*C*H$_3$)$_2$), 23.43 (CH(*C*H$_3$)$_2$) ppm. The resonance for the *i*-*C*$_6$H$_5$ carbon atom could not be observed, possibly due to signal broadening.

^{31}P NMR (202.5 MHz, 300 K, benzene-d_6): δ −32.3 (br) ppm.

^{11}B NMR (160.5 MHz, 300 K, benzene-d_6): δ –24.5 (br) ppm.

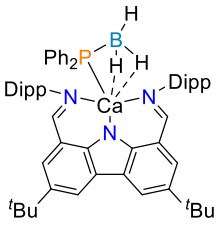

[{Carb}Ca(PPh$_2$.BH$_3$)] (3). In a Schlenk flask, [{Carb}Ca(N{SiMe$_3$}$_2$)$_2$] (300 mg, 0.35 mmol) and HPPh$_2$.BH$_3$ (70 mg, 0.35 mmol) were dissolved in petroleum ether (30 mL), generating a yellow solution. Stirring at room temperature overnight followed by evacuation of the volatiles then gave the desired product as a yellow solid. Yield: 300 mg (97%). Despite repeated attempts, this compound could not be recrystallised.

^{1}H NMR (500.1 MHz, 300 K, toluene-d_8): δ 8.57 (br s, 2H, C*H*-Carb), 8.31 (s, 2H, C*H*=N), 7.52 (br s, 2H, C*H*-Carb), 7.14-6.91 (m, 16H, C$_6$*H*$_3$-Dipp + C$_6$*H*$_5$), 3.01 (hept, $^{3}J_{H\text{-}H}$ = 6.0, 4H, C*H*(CH$_3$)$_2$), 1.46 (s, 18H, C(C*H*$_3$)$_3$), 1.21 (d, $^{3}J_{H\text{-}H}$ = 6.6, 12H, CH(C*H*$_3$)$_2$), 1.02 (d, $^{3}J_{H\text{-}H}$ = 6.8, 12H, CH(C*H*$_3$)$_2$) ppm. The resonances for boron-bound H atoms could not be detected.

^{13}C{^{1}H} NMR (125.8 MHz, 300 K, toluene-d_8): δ 173.83 (*C*H=N), 150.20 (Ar-*C*), 148.52 (Ar-*C*), 140.17 (br s, *i*-*C*$_6$H$_5$), 140.14 (*C*$_4$-Carb), 137.95 (Ar-*C*), 134.52 (d, $^{2}J_{C\text{-}P}$ = 14.6, *o*-*C*$_6$H$_5$), 131.86 (*C*$_2$-Carb), 129.56 (Ar-*C*), 127.93 (d, $^{3}J_{C\text{-}P}$ = 6.1, *m*-*C*$_6$H$_5$), 127.22 (Ar-*C*), 125.98 (Ar-*C*) 124.76 (*p*-*C*$_6$H$_5$),

123.12 (Ar-*C*), 119.47 (Ar-*C*), 34.96 (*C*(CH_3)$_3$), 32.51 (C(*C*H_3)$_3$), 29.92 (*C*H(CH_3)$_2$), 25.82 (CH(*C*H_3)$_2$), 23.58 (CH(*C*H_3)$_2$) ppm.

^{31}P NMR (202.5 MHz, 300 K, toluene-d_8): δ −41.3 (br) ppm.

^{11}B NMR (160.5 MHz, 300 K, toluene-d_8): δ –26.9 (br) ppm.

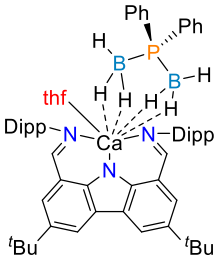

[{Carb}Ca{(BH_3)$_2$$PPh_2$}.(thf)] (4). In a Schlenk flask, [{Carb}Ca$N(SiMe_3)_2$] (400 mg, 0.47 mmol) and $HPPh_2.BH_3$ (94 mg, 0.47 mmol) were dissolved in petroleum ether (30 mL), generating a yellow solution. After 30 min, thf (1 mL) was added dropwise, generating a pale-yellow suspension. Filtration with a filter cannula followed by concentration to ca. 3 mL gave a concentrated solution which, upon storage at – 30 °C, yielded in a crop of pale-yellow crystals. Isolated yield: 80 mg (70% based on B, 35% based on Ca).

^{1}H NMR (400.1 MHz, 302 K, benzene-d_6): δ 8.70 (d, $^4J_{H\text{-}H}$ = 2.0, 2H, C*H*-Carb), 8.50 (s, 2H, C*H*=N), 7.60 (d, $^4J_{H\text{-}H}$ = 2.1, C*H*-Carb), 7.38 (m, 4H, C_6H_5), 7.03-6.89 (m, 12H, C_6H_3-Dipp + C_6H_5), 3.42 (m, 4H, OCH_2), 3.25 (hept, $^3J_{H\text{-}H}$ = 6.6, 4H, C*H*(CH_3)$_2$), 1.40 (s, 18H, C(CH_3)$_3$), 1.34 (d, $^3J_{H\text{-}H}$ = 6.8, 12H, CH(CH_3)$_2$), 1.30 (m, 4H, OCH_2CH_2), 1.02 (d, $^3J_{H\text{-}H}$ = 6.7, 12H, CH(CH_3)$_2$) ppm. The resonances for boron-bound H atoms could not be detected.

^{13}C{^{1}H} NMR (100.6 MHz, 302 K, benzene-d_6): δ 173.43 (*C*H=N), 150.88 (Ar-*C*), 148.04 (Ar-*C*), 140.04 (Ar-*C*), 139.61 (br, *i*-C_6H_5), 134.41 (br, *o*-C_6H_5), 134.24 (Ar-*C*), 134.08 (br, C_6H_5), 132.05 (*C*$_2$-Carb), 128.86 (Ar-*C*), 128.80 (Ar-*C*), 128.60 (Ar-*C*), 126.62 (Ar-*C*), 124.29 (br, C_6H_5), 122.83 (Ar-*C*), 119.15 (Ar-*C*), 68.08 (O*C*H_2), 34.56 (*C*(CH_3)$_3$), 32.13 (C(*C*H_3)$_3$), 29.20 (*C*H(CH_3)$_2$), 25.73 (OCH_2CH_2), 23.17 (CH(*C*H_3)$_2$) ppm.

^{31}P NMR (202.5 MHz, 302 K, benzene-d_6): δ −22.6 (br) ppm

^{11}B NMR (160.5 MHz, 302 K, benzene-d_6): δ –32.5 (br) ppm

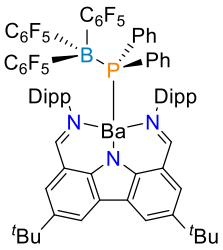

[{Carb}Ba{PPh_2.B(C_6F_5)$_3$}] (5). In a Schlenk flask, [{Carb}Ba$N(SiMe_3)_2$] (300 mg, 0.32 mmol) was dissolved in toluene (20 mL) and cooled to – 78 °C. A solution of $HPPh_2.B(C_6F_5)_3$ (220 mg, 0.32 mmol) in toluene (10 mL) was added dropwise over 10 min, generating a yellow solution. The cold bath was removed and the solution was stirred at room temperature for 1 h. The volatiles were removed and the resulting residue was washed with hexanes (2×5 mL) and dried to constant weight to give the title compound as a bright yellow solid. Yield: 350 mg (74%). The NMR could not be collected in deuterated benzene due to the relative insolubility of the compound in this solvent. Instead, in order to increase S/N in the spectrum, a NMR tube could be heated before analysis to increase the solubility of the compound in toluene-d_8.

^{1}H NMR (300.1 MHz, 298 K, toluene-d_8): δ 8.30 (d, $^4J_{H\text{-}H}$ = 1.7, 2H, C*H*-Carb), 8.23 (s, 2H, C*H*=N), 7.40 (d, $^4J_{H\text{-}H}$ = 2.0, 2H, C*H*-Carb), 7.13-6.97 (m, 6H, C_6H_3-Dipp), 6.61-6.50 (m, 10H, C_6H_5), 2.92 (hept,

$^{3}J_{H\text{-}H}$ = 6.7, 4H, C*H*(CH$_3$)$_2$), 1.39 (s, 18H, C(C*H*$_3$)$_3$), 1.02 (d, $^{3}J_{H\text{-}H}$ = 6.5, 12H, CH(C*H*$_3$)$_2$), 0.94 (d, $^{3}J_{H\text{-}H}$ = 6.7, 12H, CH(C*H*$_3$)$_2$) ppm.

^{13}C{^{1}H} NMR (100.6 MHz, 298 K, toluene-d_8): δ 171.56 (*C*H=N), 146.89 (Ar-*C*), 146.80 (Ar-*C*), 149.05 (dm, *C*$_6$F$_5$),140.76 (*C*$_6$F$_5$), 140.48 (Ar-*C*), 140.02 (Ar-*C*), 138.48 (Ar-*C*), 137.80 (*C*$_6$F$_5$), 134.58 (d, $^{1}J_{C\text{-}P}$ = 16.8, *i*-*C*$_6$H$_5$), 133.29 (d, $^{2}J_{C\text{-}P}$ = 14.4, *o*-*C*$_6$H$_5$), 132.02 (Ar-*C*), 129.56 (Ar-*C*, obscured by deuterated solvent), 127.38 (d, $^{3}J_{C\text{-}P}$ = 4.0, *m*-*C*$_6$H$_5$), 128.55 (Ar-*C*), 125.28 (Ar-*C*), 123.64 (*p*-*C*$_6$H$_5$), 123.46 (Ar-*C*), 119.45 (Ar-*C*), 34.84 (*C*(CH$_3$)$_3$), 32.41 (C(*C*H$_3$)$_3$), 29.41 (*C*H(CH$_3$)$_2$), 25.48 (CH(*C*H$_3$)$_2$), 23.81 (CH(*C*H$_3$)$_2$) ppm.

^{11}B NMR (128.4 MHz, 298 K, toluene-d_8): δ –12.6 (br s) ppm.

^{31}P NMR (162.0 MHz, 298 K, toluene-d_8): δ −9.6 (br s) ppm.

^{19}F NMR (376.5 MHz, 298 K, toluene-d_8): δ –128.10 (m, 6F, *o*-*F*), −160.25 (t, $^{3}J_{FF}$ = 21.0 Hz, 3F, *p*-*F*), –164.79 (br s, 6F, *m*-*F*) ppm.

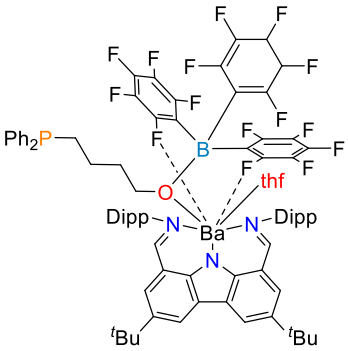

[{Carb}Ba{O(B{C$_6$F$_5$}$_3$)(CH$_2$)$_4$PPh$_2$}.(thf)] (6). Thf (1 mL) was added dropwise to a suspension of [{Carb}Ba{PPh$_2$.B(C$_6$F$_5$)$_3$}] (**5**; 168 mg, 0.112 mmol) in petroleum ether (20 mL) and the reaction mixture was stirred until the suspension turned to a yellow solution. The solution was stirred for an additional 1 h, and then concentrated until solid started to crash out of solution. The solution was then warmed 50 °C to drive the solids back into solution, and slowly cooled to room temperature. After several days, small yellow crystals of the title compound were deposited on the walls of the flask. Isolated yield: 112 mg (61%).

^{1}H NMR (400.2 MHz, 298 K, benzene-d_6): δ 8.68 (d, $^{4}J_{H\text{-}H}$ = 1.9, 2H, C*H*-Carb), 8.47 (s, 2H, C*H*=N), 7.73 (d, $^{4}J_{H\text{-}H}$ = 2.1, 2H, C*H*-Carb), 7.34 (m, 4H, C$_6$*H*$_5$), 7.13-6.97 (m, 10H, C$_6$*H*$_5$+ C$_6$*H*$_3$-Dipp), 3.00 (m, 6H, C*H*(CH$_3$)$_2$ + PCH$_2$CH$_2$CH$_2$C*H*$_2$), 2.85 (m, 4H, OC*H*$_2$-thf), 1.52 (s, 18H, C(C*H*$_3$)$_3$), 1.22 (d, $^{3}J_{H\text{-}H}$ = 6.6, 6H, CH(C*H*$_3$)$_2$), 1.06 (m, 6H, PCH$_2$C*H*$_2$ + OCH$_2$C*H*$_2$-thf), 1.00 (d, $^{3}J_{H\text{-}H}$ = 6.6, 6H, CH(C*H*$_3$)$_2$), 0.92 (d, $^{3}J_{H\text{-}H}$ = 6.6, 12H, CH(C*H*$_3$)$_2$, two overlapping but inequivalent resonances), 0.56 (br m, 2H, PCH$_2$CH$_2$C*H*$_2$), −0.28 (br m, 2H, PC*H*$_2$) ppm. Resonances for hydrolysed {Carb}H could also be seen.

^{13}C{^{1}H} NMR (100.6 MHz, 298 K, benzene-d_6): δ 172.31 (*C*H=N), 148.81 (Ar-*C*),) 148.57 (dm, *C*$_6$F$_5$), 147.57 (Ar-*C*), 140.46 (*C*$_6$F$_5$), 139.92 (Ar-*C*), 139.69 (d, $^{1}J_{C\text{-}P}$ = 14.5, *i*-*C*$_6$H$_5$), 139.56 (dm, *C*$_6$F$_5$), 137.30 (dm, *C*$_6$F$_5$), 132.97 (Ar-*C*), 132.76 (d, $^{2}J_{C\text{-}P}$ = 18.6, *o*-*C*$_6$H$_5$), 128.72 (d, ^{3}$_{C\text{-}P}$ = 6.6, *m*-*C*$_6$H$_5$), 128.66 (Ar-*C*), 128.18 (*p*-*C*$_6$H$_5$), 127.36 (Ar-*C*), 124.81 (Ar-*C*), 124.32 (Ar-*C*), 123.34 (Ar-*C*), 120.27 (Ar-*C*), 67.86 (O*C*H$_2$-thf), 64.54 (PCH$_2$CH$_2$CH$_2$*C*H$_2$), 34.69 (*C*(CH$_3$)$_3$), 32.06 (C(*C*H$_3$)$_3$), 31.16 (d, $^{3}J_{C\text{-}P}$ = 12.8, PCH$_2$CH$_2$*C*H$_2$), 29.30 (*C*H(CH$_3$), 28.58 (*C*H(CH$_3$)), 28.33 (d, $^{2}J_{C\text{-}P}$ = 12.6, PCH$_2$*C*H$_2$), 26.15 (CH(*C*H$_3$)$_2$), 25.13 (OCH$_2$*C*H$_2$-thf), 24.84 (CH(*C*H$_3$)$_2$), 23.66 (CH(*C*H$_3$)$_2$), 22.30 (CH(*C*H$_3$)$_2$), 21.55 (d, $^{1}J_{C\text{-}P}$ =18.9, P*C*H$_2$) ppm.

^{11}B NMR (128.4 MHz, 298 K, benzene-d_6): δ –2.6 (br s) ppm.

^{31}P NMR (162.0 MHz, 298 K, benzene-d_6): δ −18.8 (s) ppm.

^{19}F NMR (376.5 MHz, 298 K, benzene-d_6): δ –132 to –135 (br m, 4F), –156 to –159 (m, 6 F), −134.06 (br d, 1F, *o*-F), −161 to –165 (m, 6F,) ppm. We were unable to interpret and assign the multiple and broad resonances, including with VT NMR.

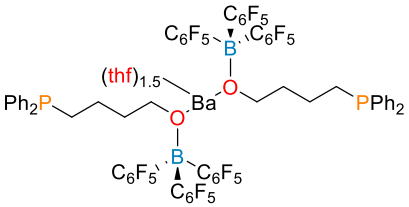

[Ba{O(B{C$_6$F$_5$}$_3$)(CH$_2$)$_4$PPh$_2$}$_2$.(thf)$_{1.5}$] (7). In a Schlenk flask, [Ba{N(SiMe$_3$)$_2$}$_2$]$_2$ (150 mg, 0.16 mmol) and HPPh$_2$.B(C$_6$F$_5$)$_3$ (447 mg, 0.64 mmol) were mixed in petroleum ether (25 mL), generating a pale-yellow suspension. Thf (approx. 10 mL) was added dropwise until the suspension became a colourless solution. Removal of the volatiles followed by washing with petroleum ether (3 × 30 mL and drying under reduced pressure to constant weight gave the compound as a white solid. Yield: 384 mg (88%).

^{1}H NMR (500.1 MHz, 300 K, thf-d_8): δ 7.34 (m, 8H, C$_6$*H*$_5$), 7.23 (m, 12H, C$_6$*H*$_5$), 3.62 (m, 6H, OC*H*$_2$-thf), 3.12 (m, 4H, PCH$_2$CH$_2$CH$_2$C*H*$_2$), 2.01 (m, 4H, PCH$_2$CH$_2$C*H*$_2$), 1.77 (m, 6H, OCH$_2$C*H*$_2$-thf), 1.58 (m, 4H, PCH$_2$C*H*$_2$), 1.45 (m, 4H, PC*H*$_2$) ppm.

^{13}C{^{1}H} NMR (125.8 MHz, 300 K, thf-d_8): δ 149.22 (dm, $^1J_{C\text{-}F}$ = 239.8, *C*$_6$F$_5$), 141.00 (d, $^1J_{P\text{-}C}$ = 14.8, *i*-*C*$_6$H$_5$), 139.17 (dm, $^1J_{C\text{-}F}$ = 213.8, *C*$_6$F$_5$), 137.23 (dm, $^1J_{C\text{-}F}$ = 226.2, *C*$_6$F$_5$), 133.61 (d, $^2J_{P\text{-}C}$ = 17.1, *o*-*C*$_6$H$_5$), 129.47 (d, $^3J_{P\text{-}C}$ = 18.5, *m*-*C*$_6$H$_5$), 128.98 (*p*-*C*$_6$H$_5$), 126.41 (br, *C*$_6$F$_5$), 68.38 (O*C*H$_2$-thf), 64.45 (PCH$_2$CH$_2$CH$_2$*C*H$_2$), 35.15 (d, $^2J_{C\text{-}P}$ = 12.7, PCH$_2$*C*H$_2$), 29.13 (d, $^3J_{C\text{-}P}$ = 11.5, PCH$_2$CH$_2$*C*H$_2$), 26.52 (OCH$_2$*C*H$_2$-thf), 24.10 (d, $^1J_{C\text{-}P}$ = 16.5, P*C*H$_2$) ppm.

^{11}B NMR (128.4 MHz, 298 K, thf-d_8): δ –2.9 (br s) ppm.

^{31}P NMR (202.5 MHz, 300 K, thf-d_8): δ −16.1 (s) ppm.

^{19}F NMR (470.5 MHz, 300 K, thf-d_8): δ –133.26 (d, $^3J_{F\text{-}F}$ = 23.7, 12F, *o*-F), −165.50 (t, $^3J_{F\text{-}F}$ = 20.3, 6F, *p*-C$_6$F$_5$), –168.42 (m, 12F, *m*-*F*) ppm.

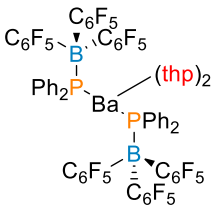

[Ba{PPh$_2$.B(C$_6$F$_5$)$_3$}$_2$.(thp)$_2$] (8). In a Schlenk tube, [Ba{N(SiMe$_3$)$_2$}$_2$]$_2$ (200 mg, 0.22 mmol) and HPPh$_2$.B(C$_6$F$_5$)$_3$ (615 mg, 0.88 mmol) were mixed in petroleum ether (30 mL), generating a pale-yellow suspension. Thp (approx. 15 mL) was added dropwise until the suspension became a colourless solution. Removal of the volatiles followed by washing with petroleum ether (3 × 30 mL) and drying under vacuum to constant weight gave the compound as a low density white solid. Yield: 715 mg (91%). Recrystallisation of a portion of the sample from a saturated solution mixture of hexanes and thp (2:1) at −30 ˚C generated crystals suitable for an X-ray diffraction study.

^{1}H NMR (500.1 MHz, 300 K, thf-d_8): δ 7.34 (m, 8H, C$_6$*H*$_5$), 7.22 (m, 12H, C$_6$*H*$_5$), 3.54 (m, 8H, OC*H*$_2$), 1.60 (m, 4H, OCH$_2$CH$_2$C*H*$_2$), 1.50 (m, 8H, OCH$_2$C*H*$_2$) ppm.

^{13}C{^{1}H} NMR (125.8 MHz, 300 K, thf-d_8): δ 149.24 (dm, $^1J_{C\text{-}F}$ = 239.8, *C*$_6$F$_5$), 141.04 (d, $^1J_{P\text{-}C}$ = 14.8, *i*-*C*$_6$H$_5$), 139.19 (dm, $^1J_{C\text{-}F}$ = 205.1, *C*$_6$F$_5$), 137.26 (dm, $^1J_{C\text{-}F}$ = 231.1, *C*$_6$F$_5$), 133.61 (d, $^2J_{P\text{-}C}$ = 18.5, *o*-

C_6H_5), 129.07 (d, $^3J_{P\text{-}C}$ = 6.4, *m*-C_6H_5), 128.94 (*p*-C_6H_5), 126.81 (br, C_6F_5), 69.22 (OCH_2), 27.80 (OCH_2CH_2), 24.68 ($OCH_2CH_2CH_2$) ppm.

^{11}B NMR (160.5 MHz, 300 K, thf-d_8): δ –2.9 (br s) ppm.

^{31}P NMR (202.5 MHz, 300 K, thf-d_8): δ −16.6 (s) ppm.

^{19}F NMR (470.5 MHz, 300 K, thf-d_8): δ –133.36 (d, $^3J_{F\text{-}F}$ = 23.7, 12F, *o*-*F*), −165.56 (t, $^3J_{F\text{-}F}$ = 20.1, 6F, *p*-*F*), –168.45 (t, $^3J_{F\text{-}F}$ = 19.8, 12F, *m*-*F*) ppm.

NMR spectra for *in situ* generated [{Carb}BaPPh$_2$.(thf)] (1.(thf)).

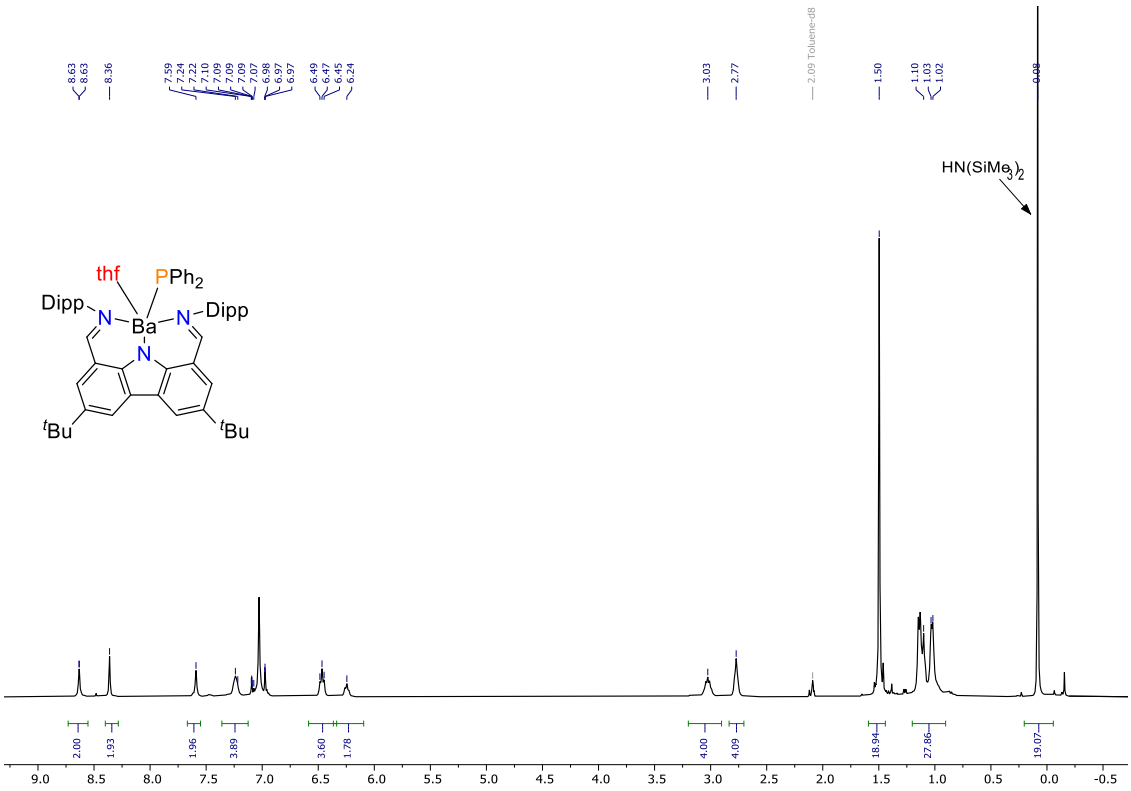

Figure S1. ^{1}H NMR spectrum (400.16 MHz, toluene-d_8, 298 K) of [{Carb}BaPPh$_2$.(thf)] (**1.(thf)**).

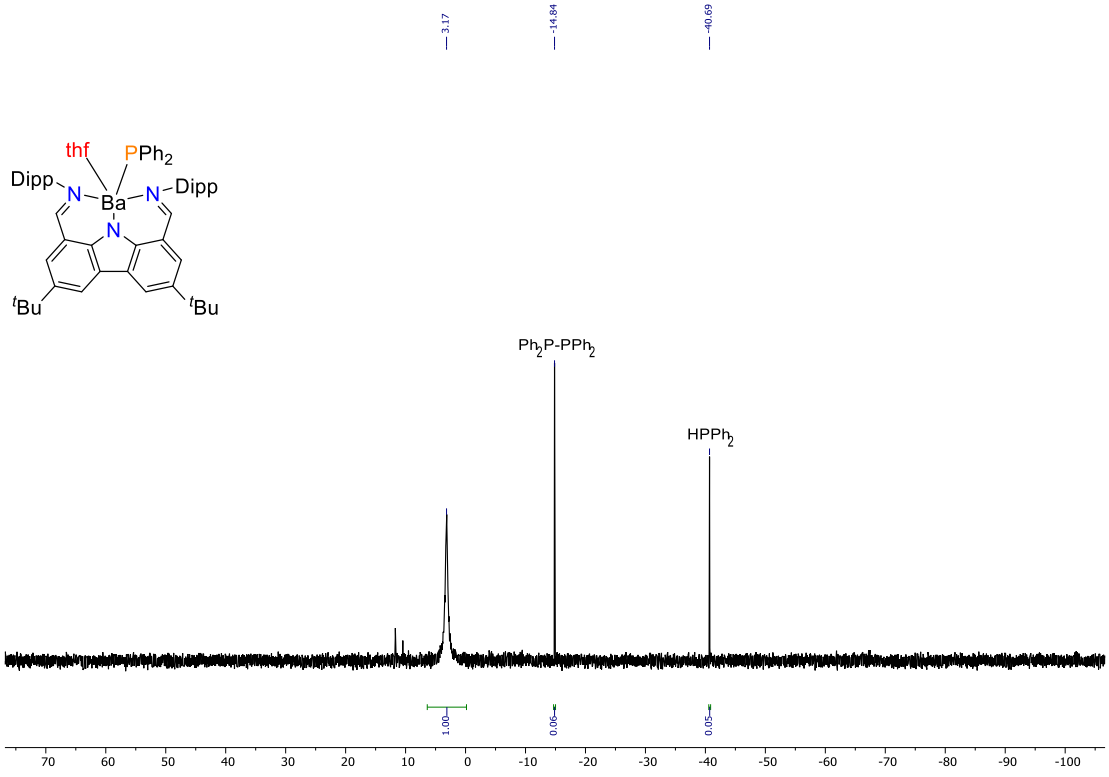

Figure S2. ^{31}P{^{1}H} NMR spectrum (161.99 MHz, toluene-d_8, 298 K) of [{Carb}BaPPh$_2$.(thf)] (**1.(thf)**).

NMR spectra for *in situ* generated [{Carb}Ba(PPh$_2$.BH$_3$)] (2)

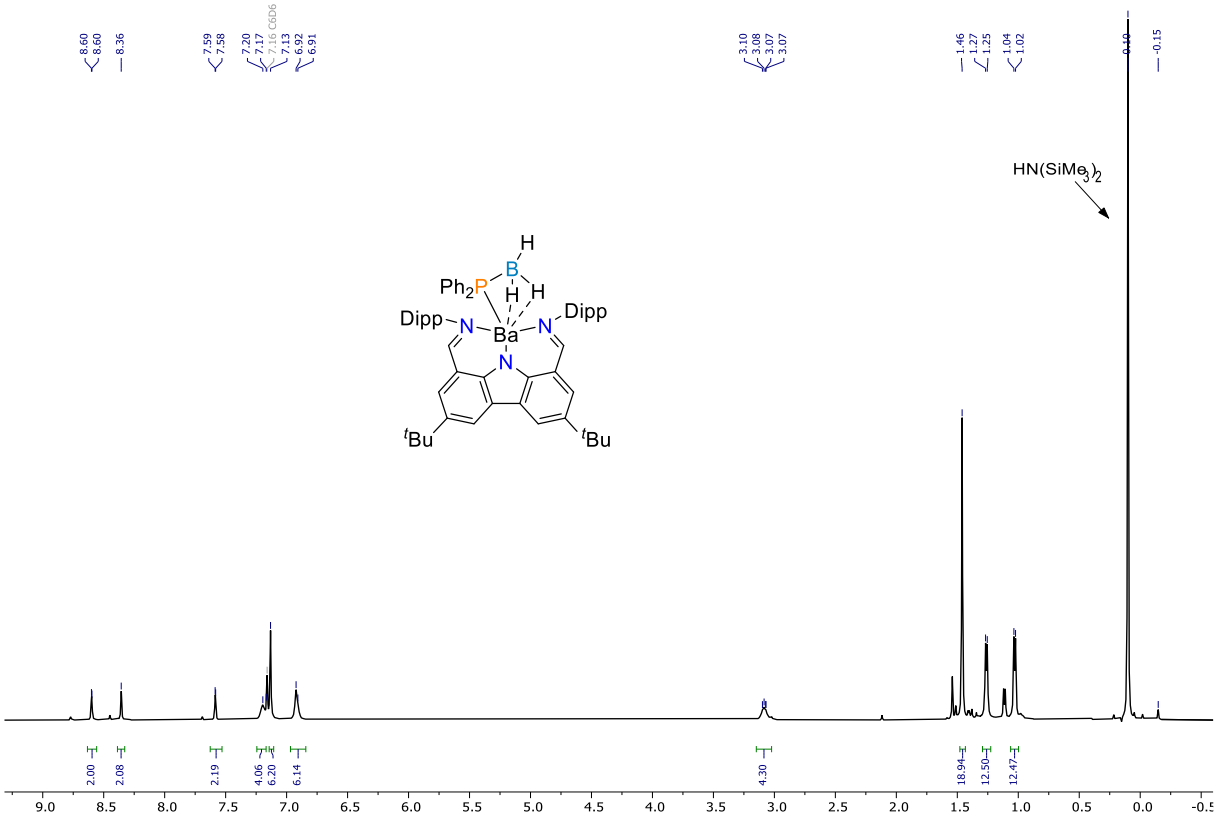

Figure S3. ^{1}H NMR spectrum (500.13 MHz, benzene-d_6, 300 K) of [{Carb}Ba(PPh$_2$.BH$_3$)] (**2**).

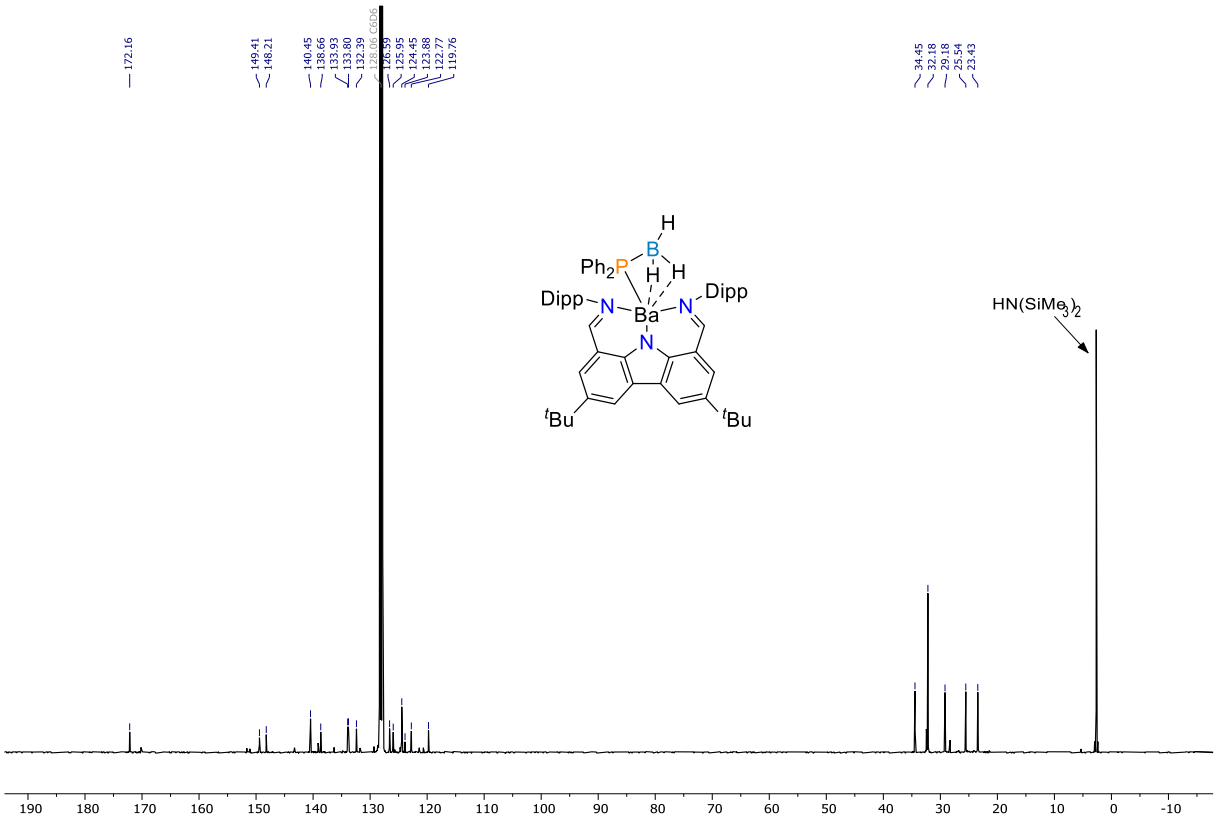

Figure S4. ^{13}C{^{1}H} NMR spectrum (100.62 MHz, benzene-d_6, 300 K) of [{Carb}Ba(PPh$_2$.BH$_3$)] (**2**).

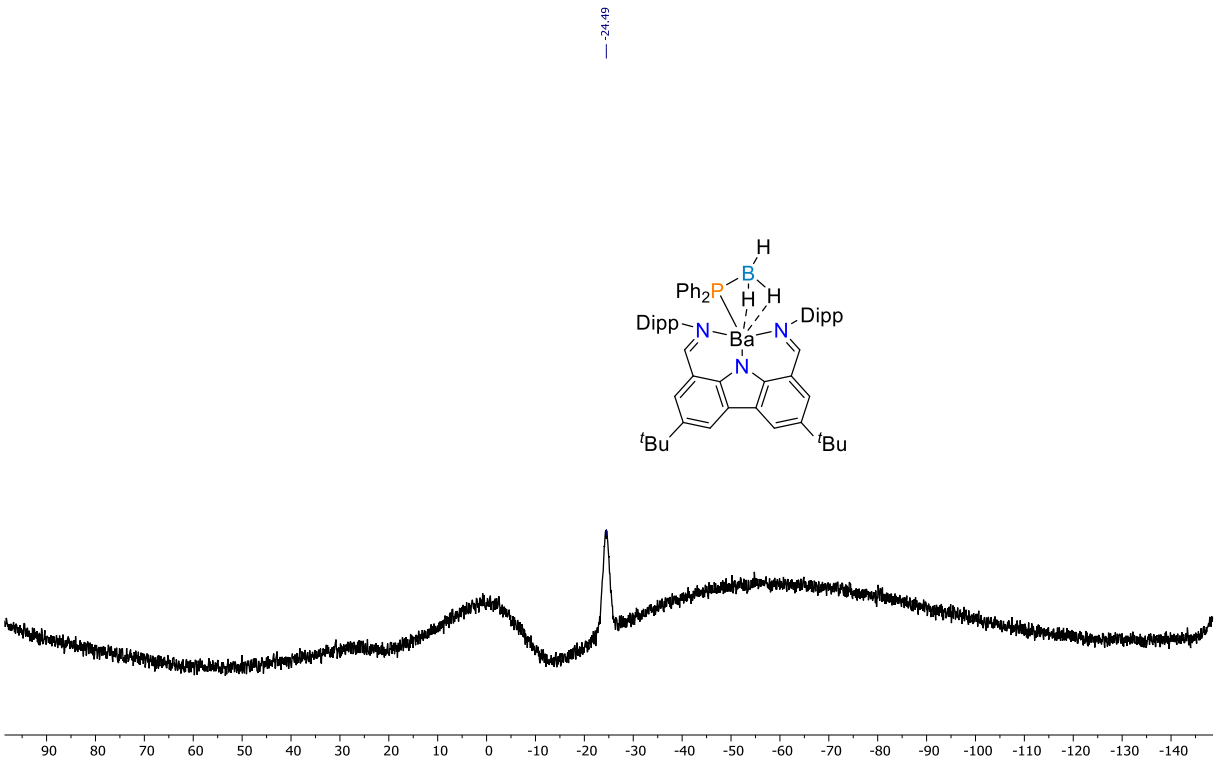

Figure S5. ^{11}B NMR spectrum (160.46 MHz, benzene-d_6, 300 K) of [{Carb}Ba($PPh_2.BH_3$)] (**2**).

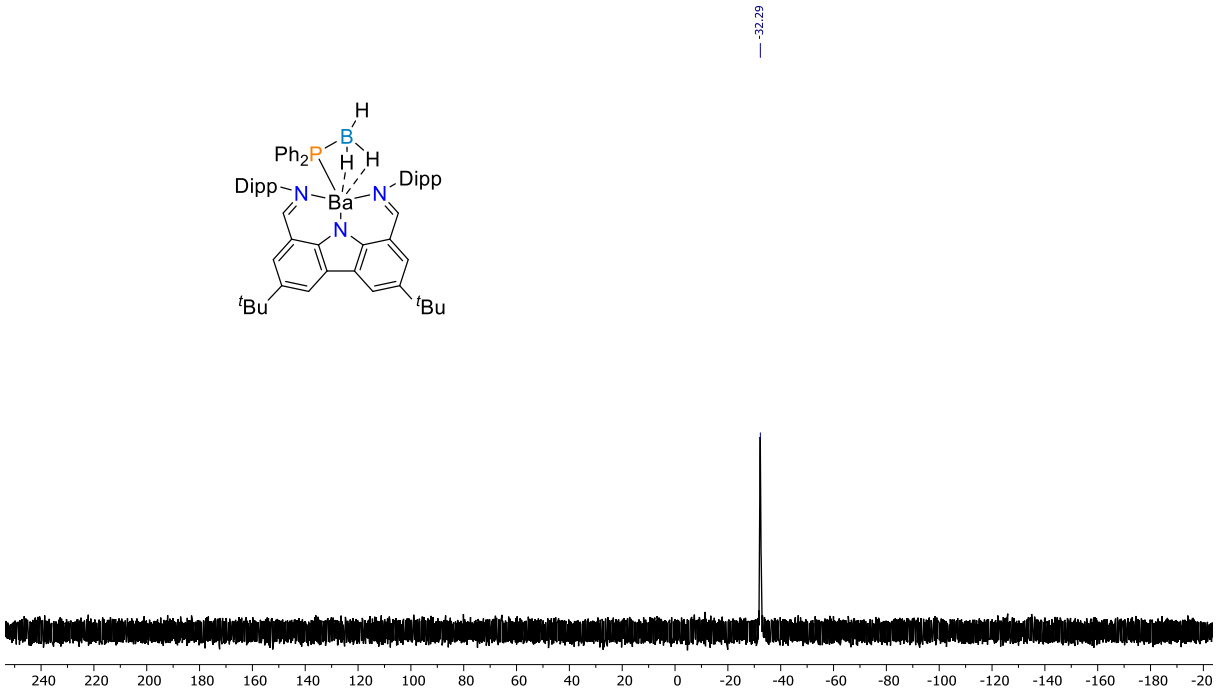

Figure S6. ^{31}P NMR spectrum (202.46 MHz, benzene-d_6, 300 K) of [{Carb}Ba($PPh_2.BH_3$)] (**2**).

NMR spectra for *in situ* generated [{Carb}Ca(PPh$_2$.BH$_3$)] (3)

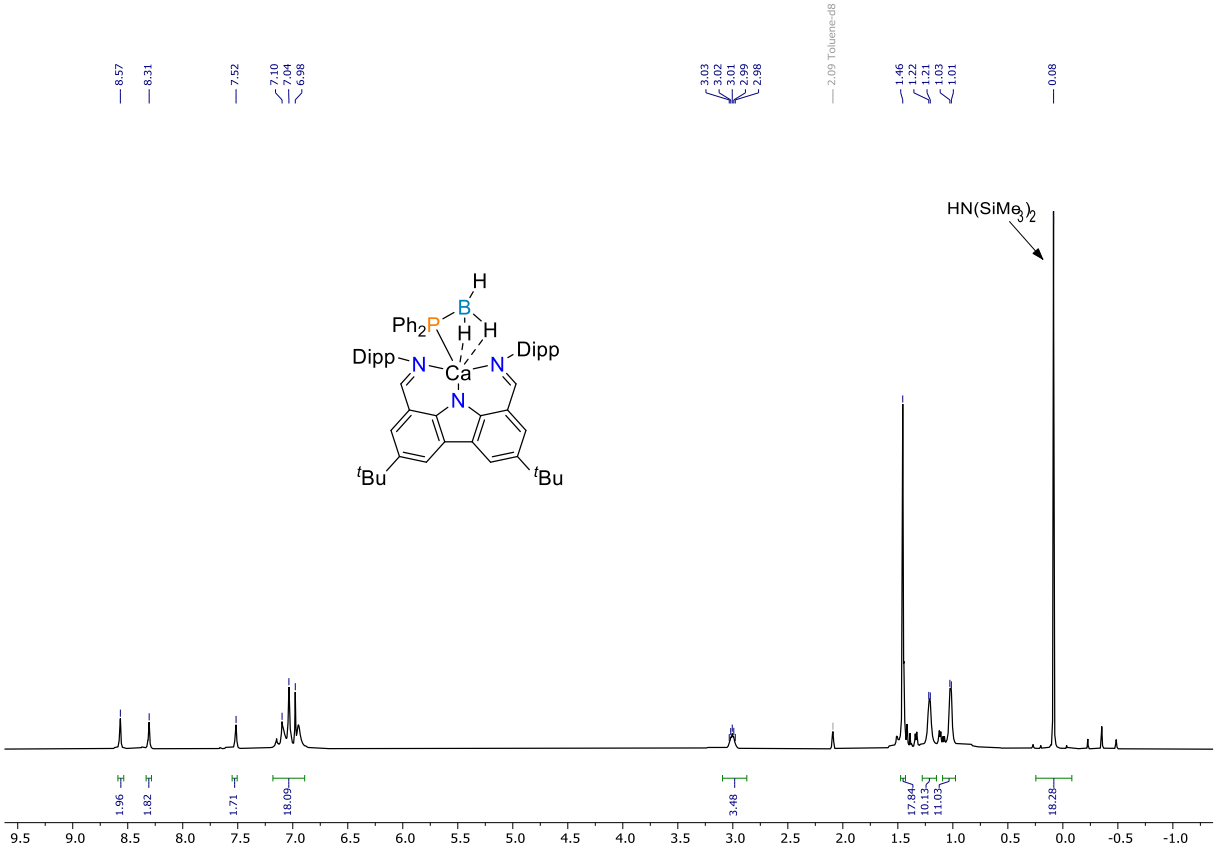

Figure S7. ^{1}H NMR spectrum (500.13 MHz, toluene-d_8, 300 K) of [{Carb}CaPPh$_2$.(thf)] (**3**).

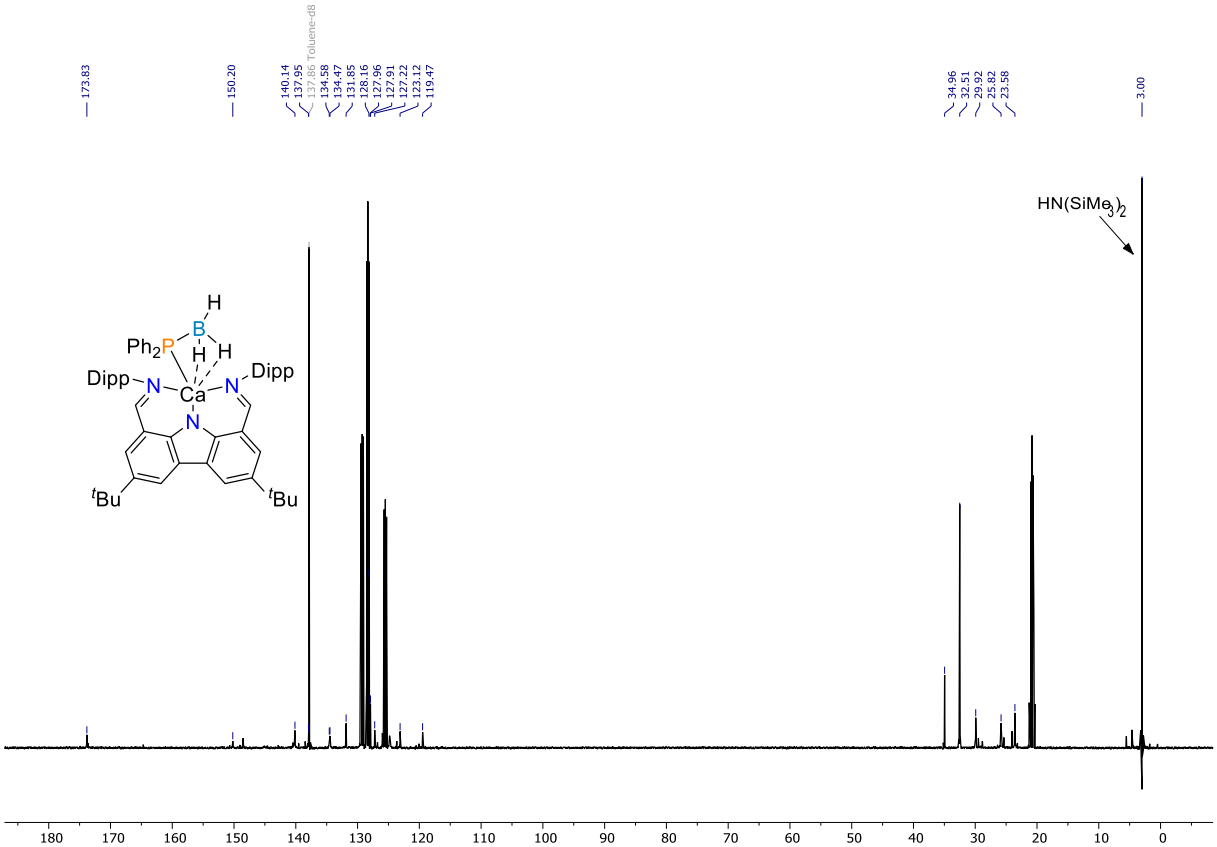

Figure S8. ^{13}C{^{1}H} NMR spectrum (125.77 MHz, toluene-d_8, 300 K) of [{Carb}CaPPh$_2$.(thf)] (**3**).

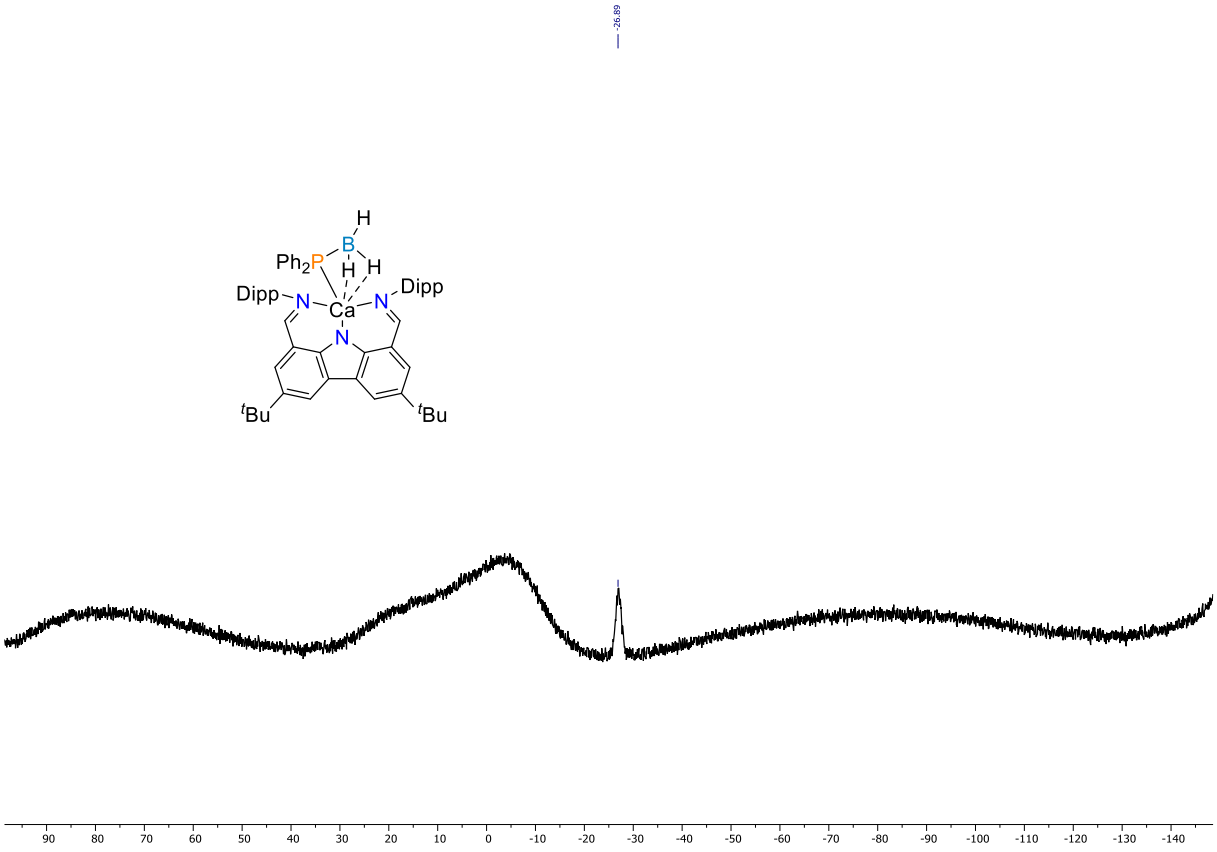

Figure S9. ^{11}B NMR spectrum (160.46 MHz, toluene-d_8, 300 K) of [{Carb}CaPPh$_2$.(thf)] (**3**).

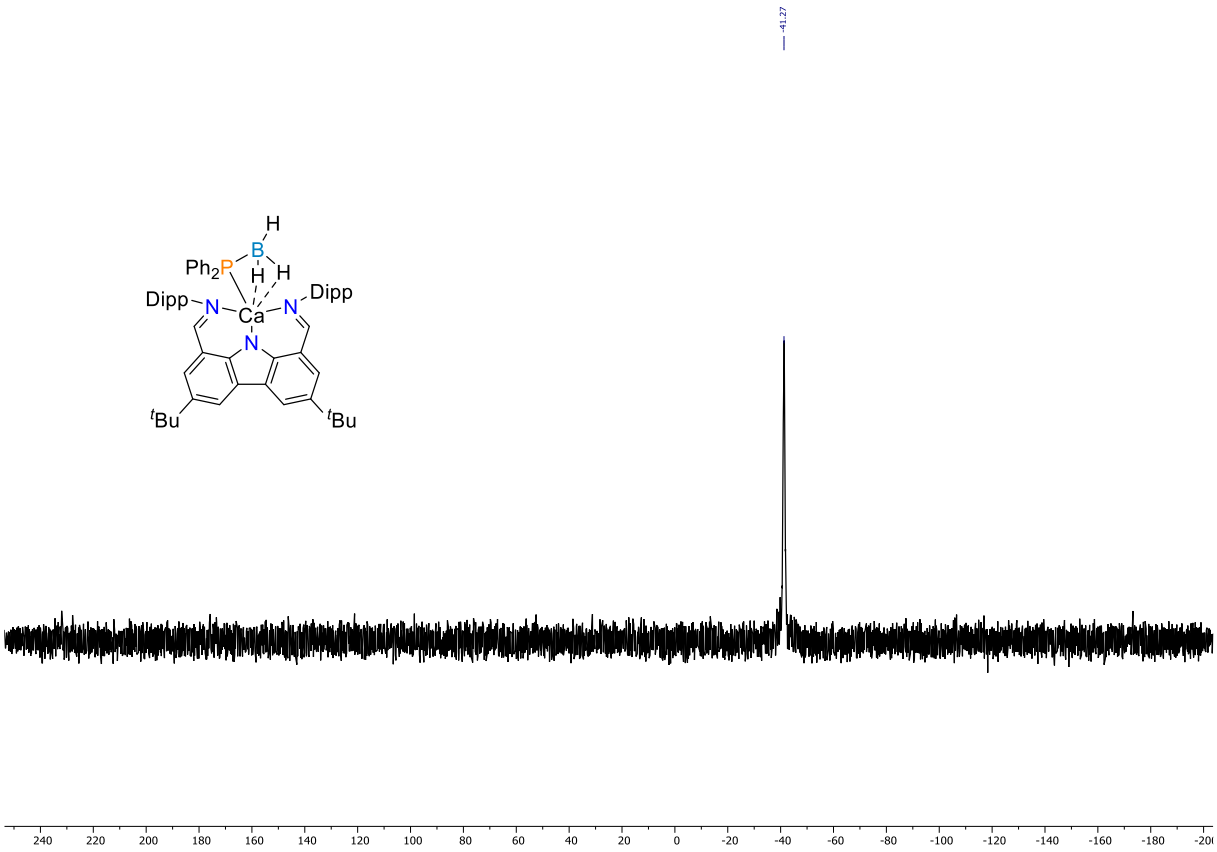

Figure S10. ^{31}P NMR spectrum (202.46 MHz, toluene-d_8, 300 K) of [{Carb}CaPPh$_2$.(thf)] (**3**).

NMR spectra for [{Carb}Ca{$(BH_3)_2PPh_2$}.(thf)] (4)

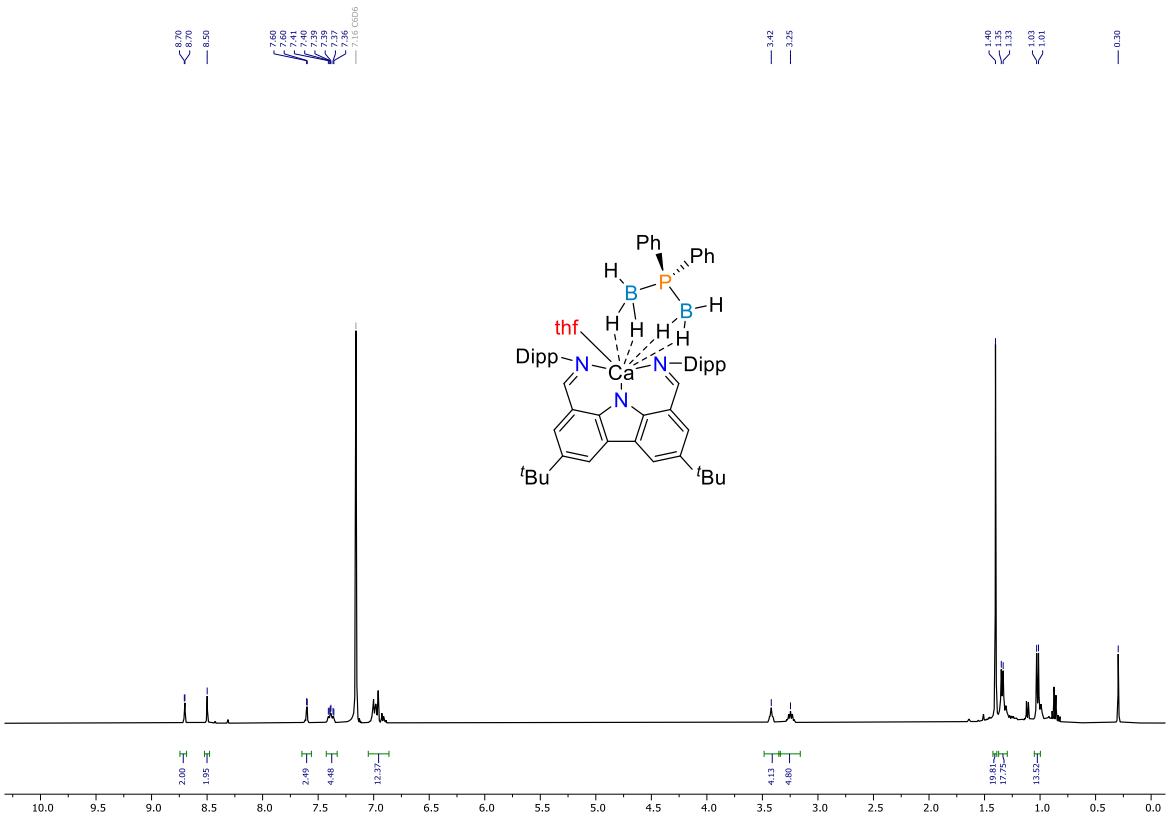

Figure S11. ^{1}H NMR spectrum (400.13 MHz, benzene-d_6, 302 K) of [{Carb}Ca{$(BH_3)_2PPh_2$}.(thf)] (**4**).

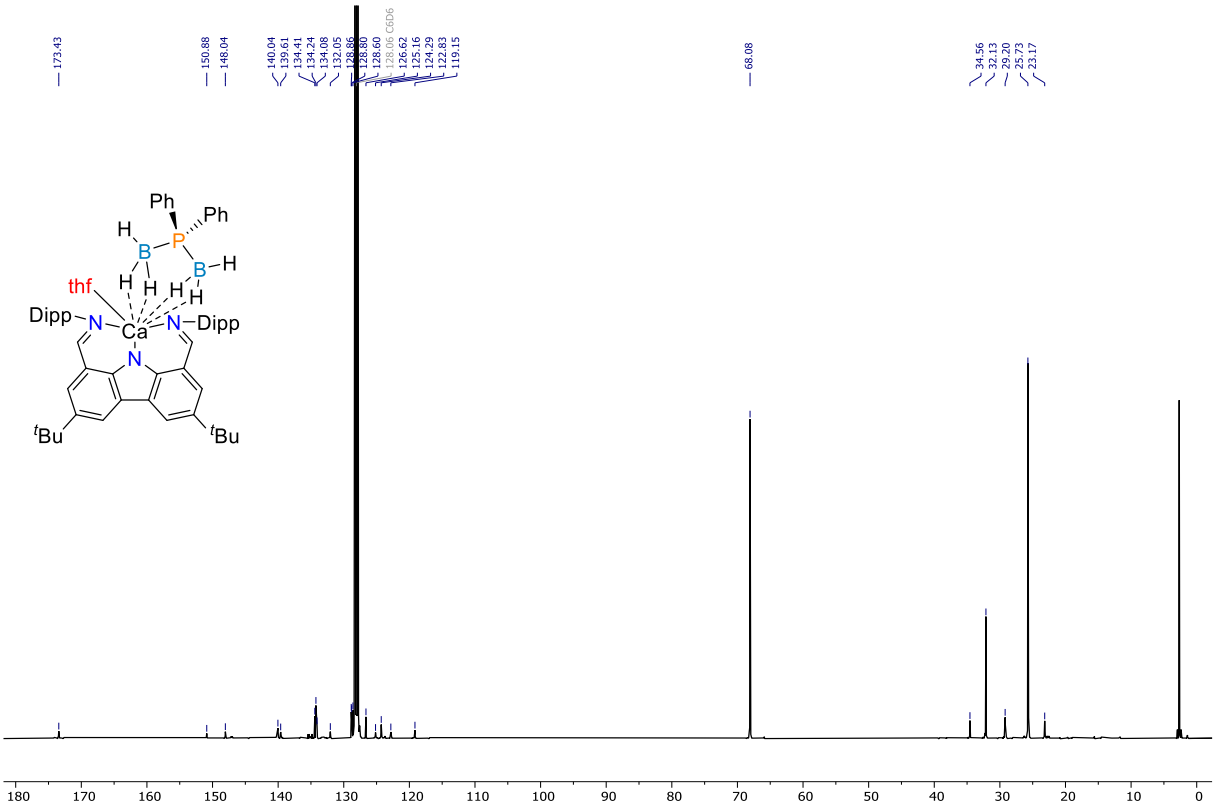

Figure S12. $^{13}C\{^{1}H\}$ NMR spectrum (100.62 MHz, benzene-d_6, 300 K) of [{Carb}Ca{$(BH_3)_2PPh_2$}.(thf)] (**4**), showing partial degradation of the compound. We were not able to record a spectrum without decomposition.

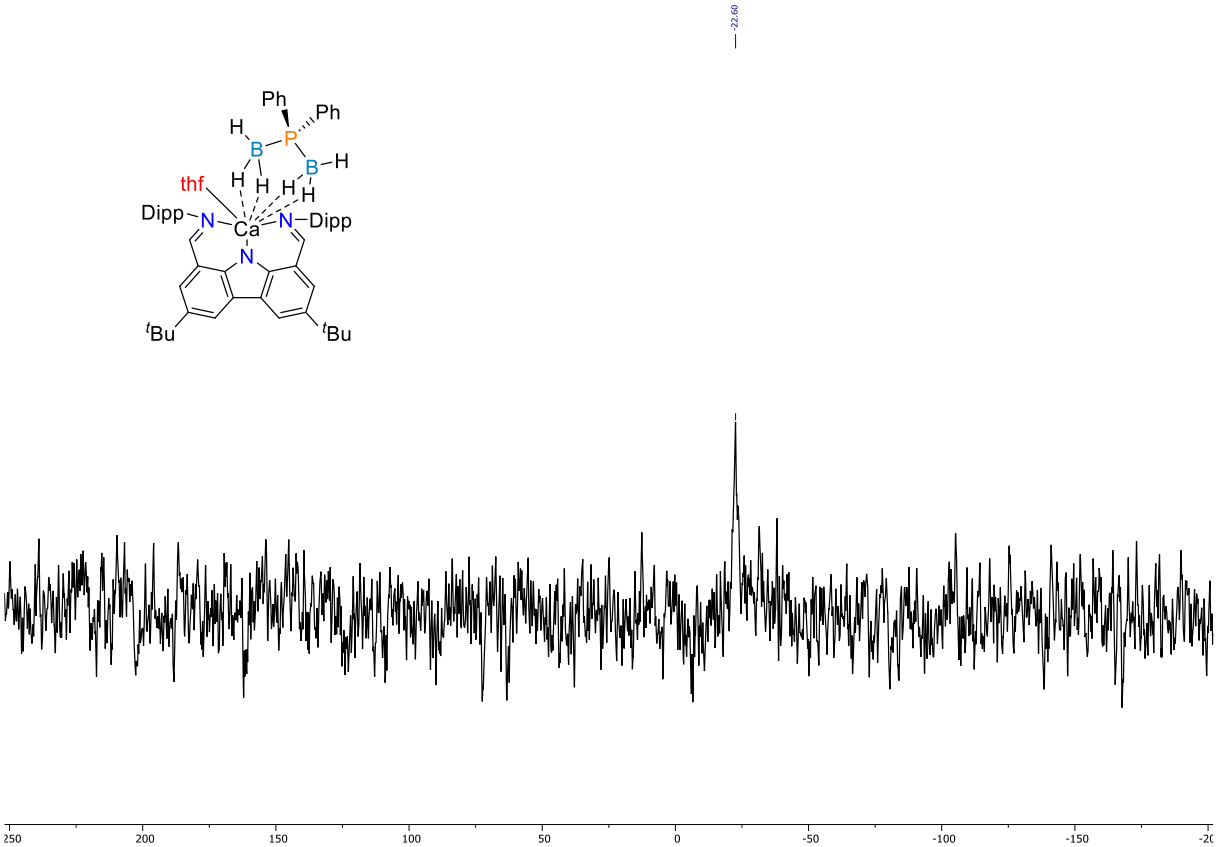

Figure S13. ^{31}P NMR spectrum (161.98 MHz, benzene-d_6, 302 K) of [{Carb}Ca{$(BH_3)_2PPh_2$}.(thf)] (**4**).

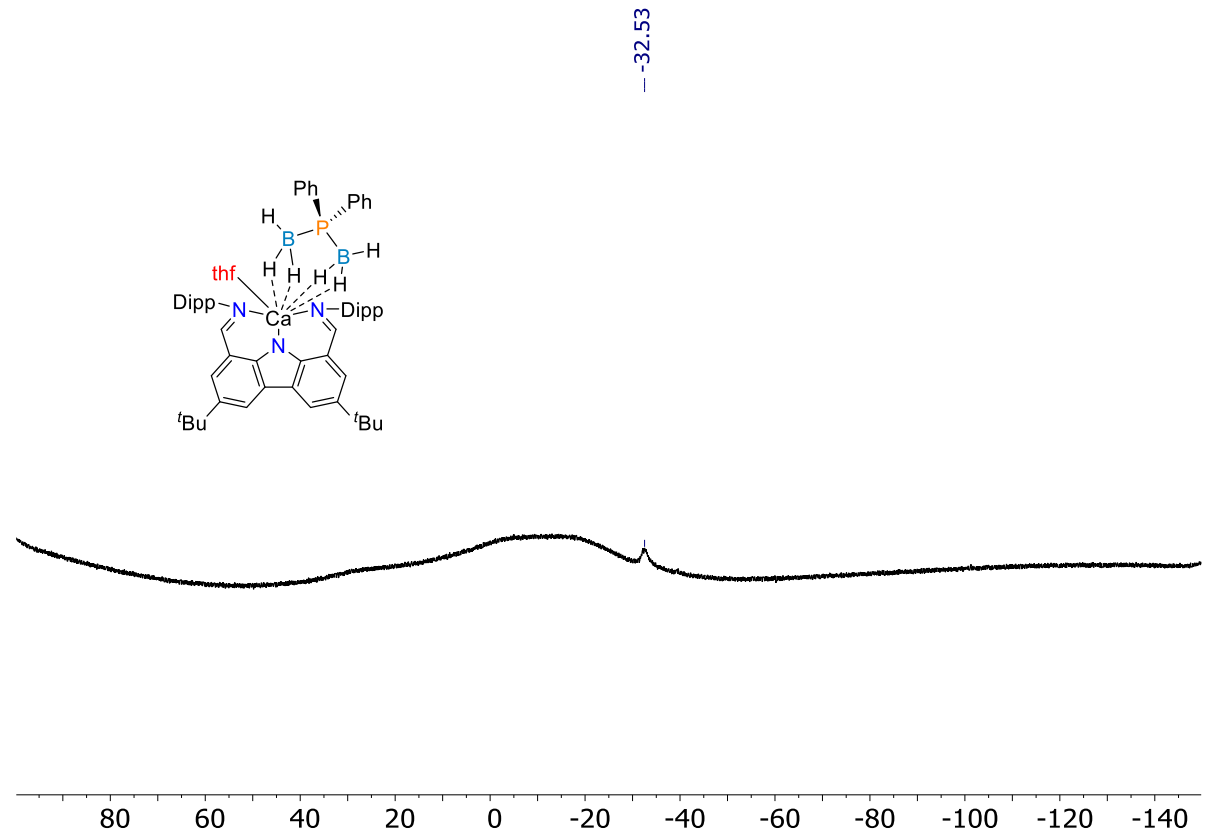

Figure S14. ^{11}B NMR spectrum (128.37 MHz, benzene-d_6, 302 K) of [{Carb}Ca{$(BH_3)_2PPh_2$}.(thf)] (**4**).

NMR spectra for [{Carb}Ba{PPh$_2$.B(C$_6$F$_5$)$_3$}] (5).

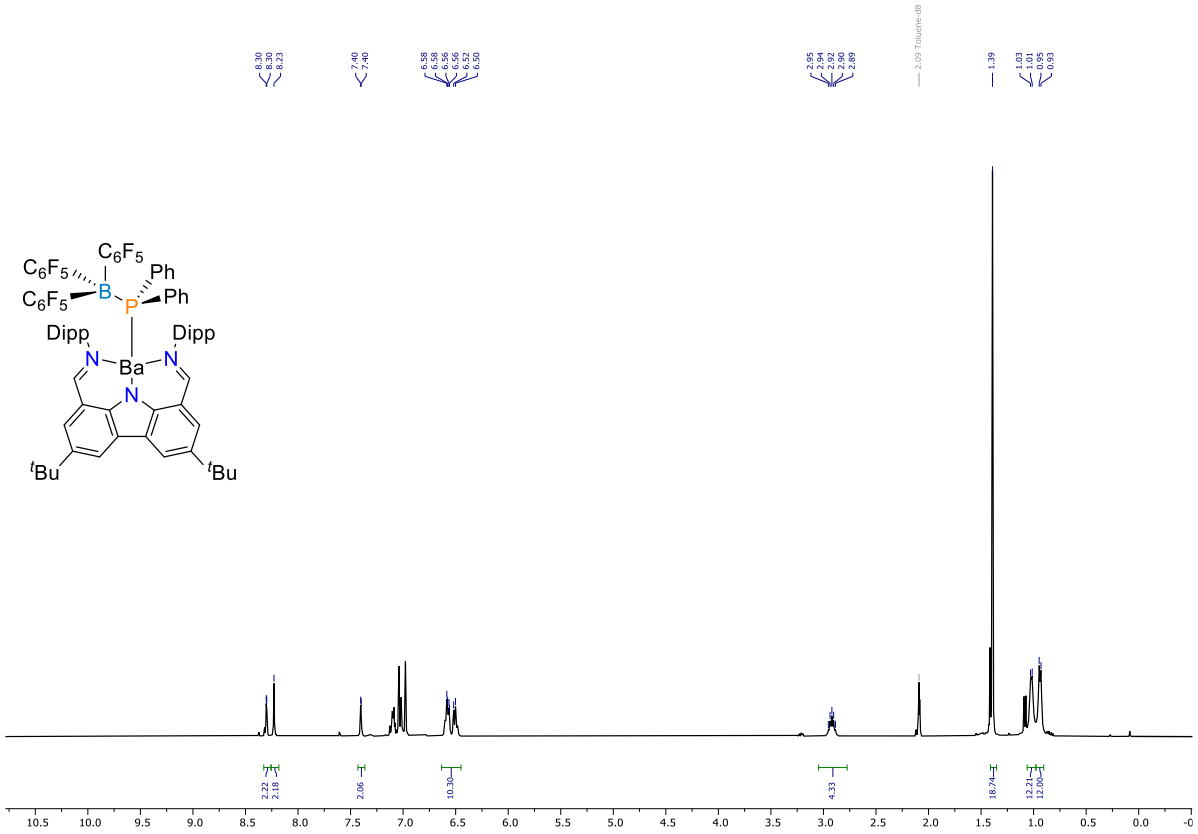

Figure S15. ^{1}H NMR spectrum (400.16 MHz, toluene-d_8, 298 K) of [{Carb}Ba{PPh$_2$.B(C$_6$F$_5$)$_3$}] (**5**).

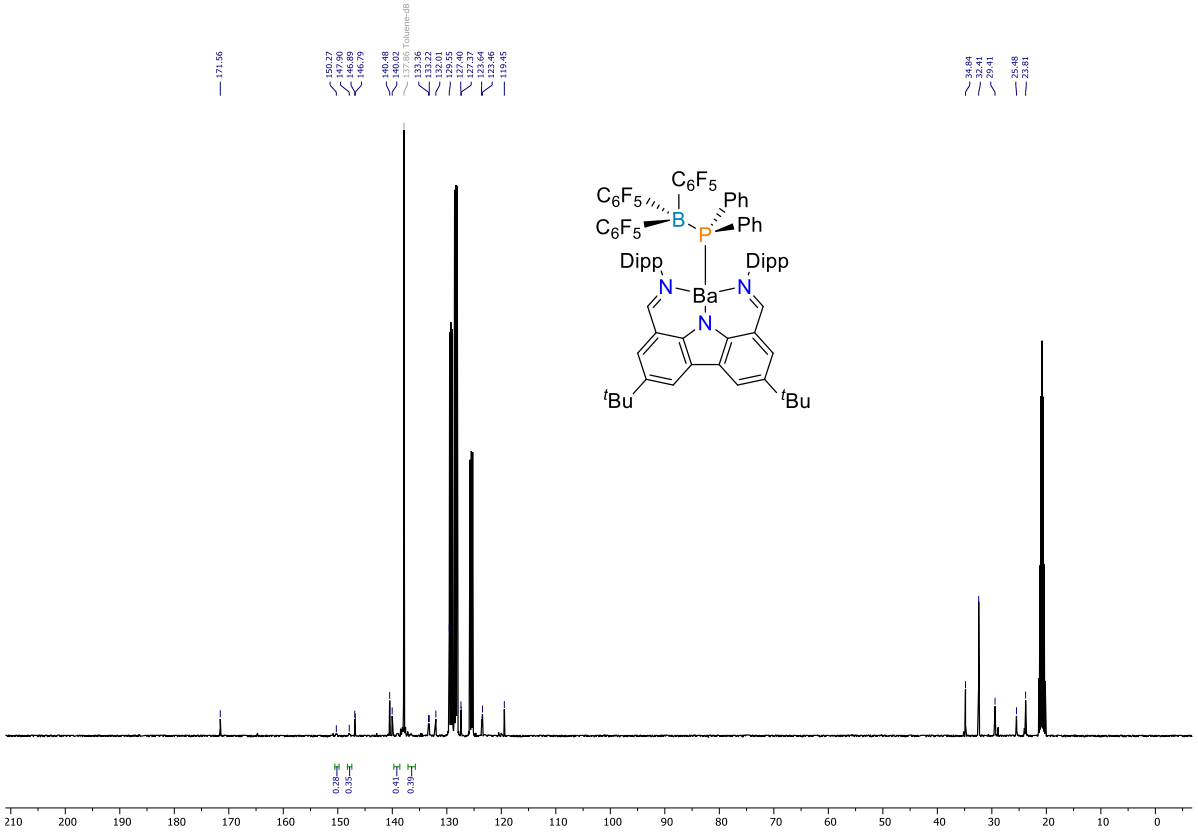

Figure S16. ^{13}C{^{1}H} NMR spectrum (100.63 MHz, toluene-d_8, 298 K) of [{Carb}Ba{PPh$_2$.B(C$_6$F$_5$)$_3$}] (**5**).

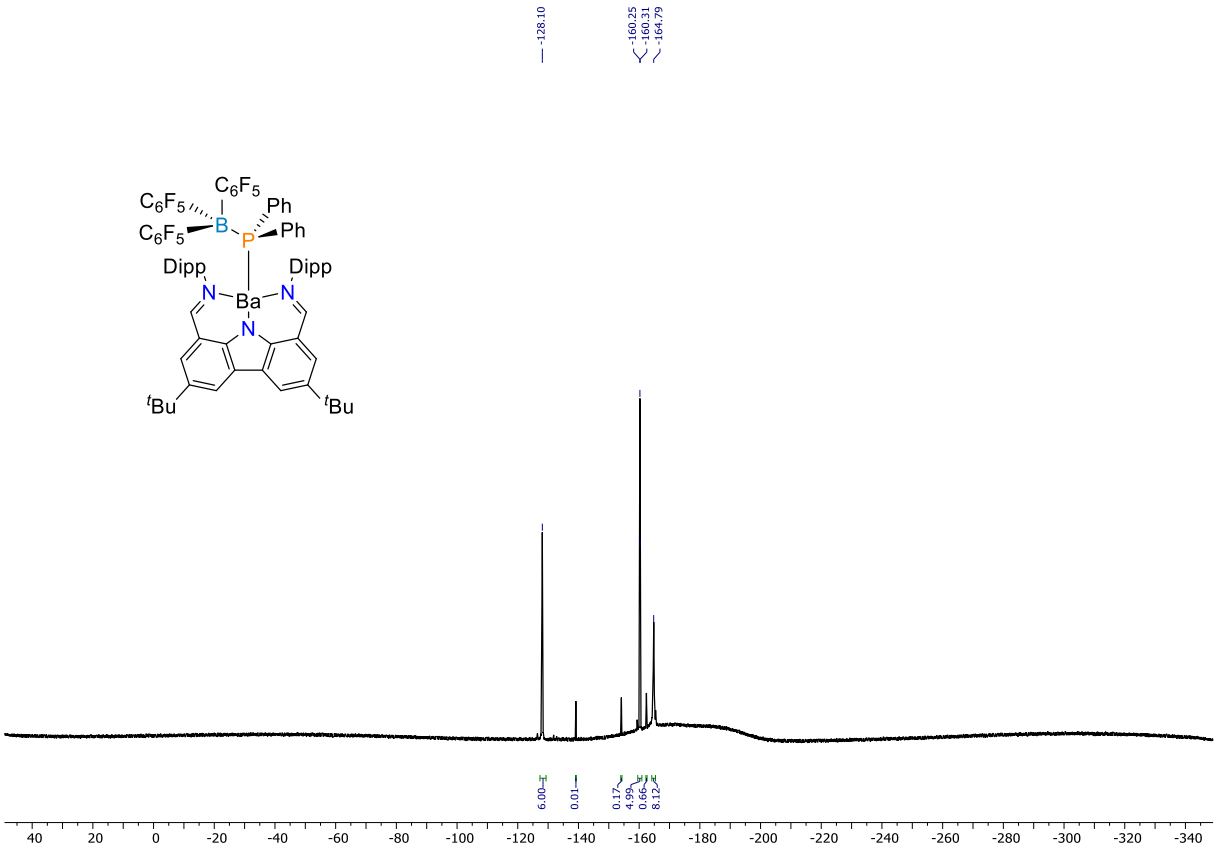

Figure S17. ^{19}F NMR spectrum (376.47 MHz, toluene-d_8, 298 K) of [{Carb}Ba{PPh_2.B(C_6F_5)$_3$}] (**5**).

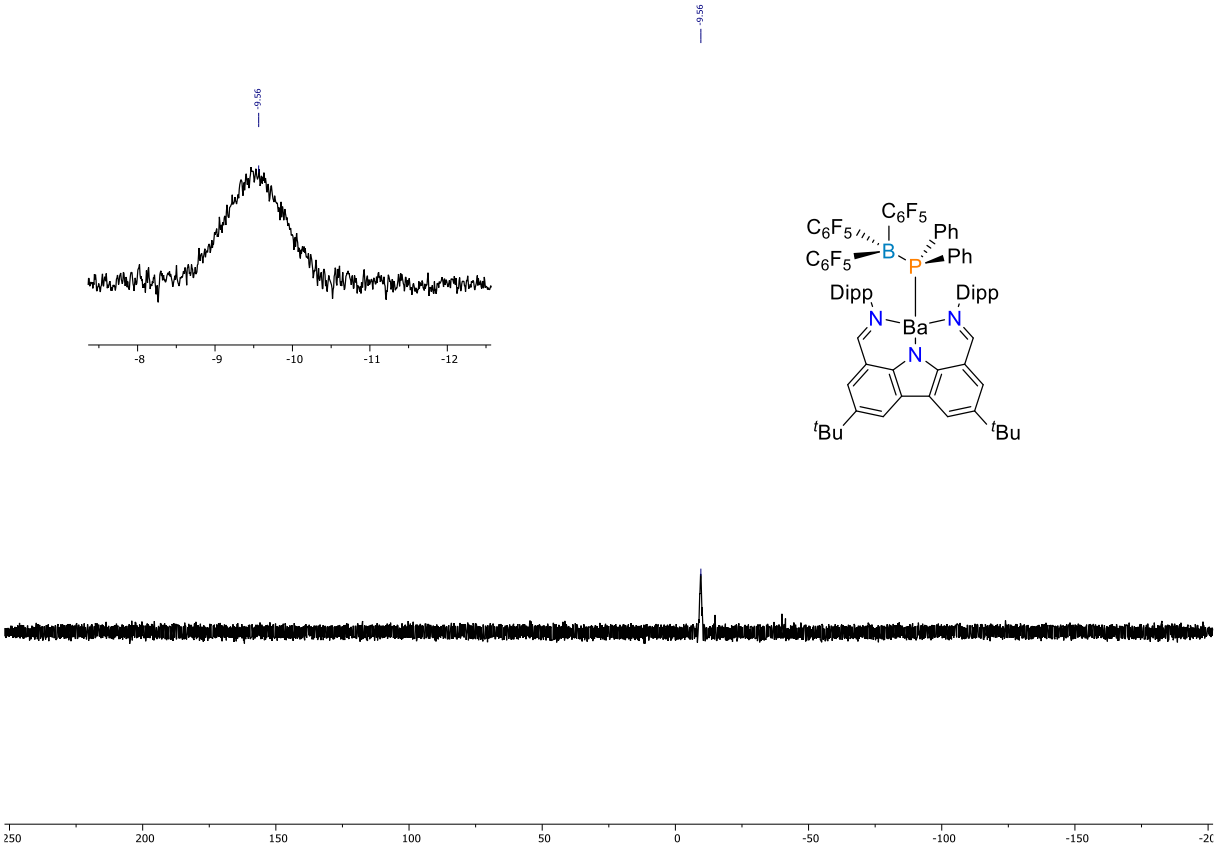

Figure S18. ^{31}P NMR spectrum (161.99 MHz, toluene-d_8, 298 K) of [{Carb}Ba{PPh_2.B(C_6F_5)$_3$}] (**5**).

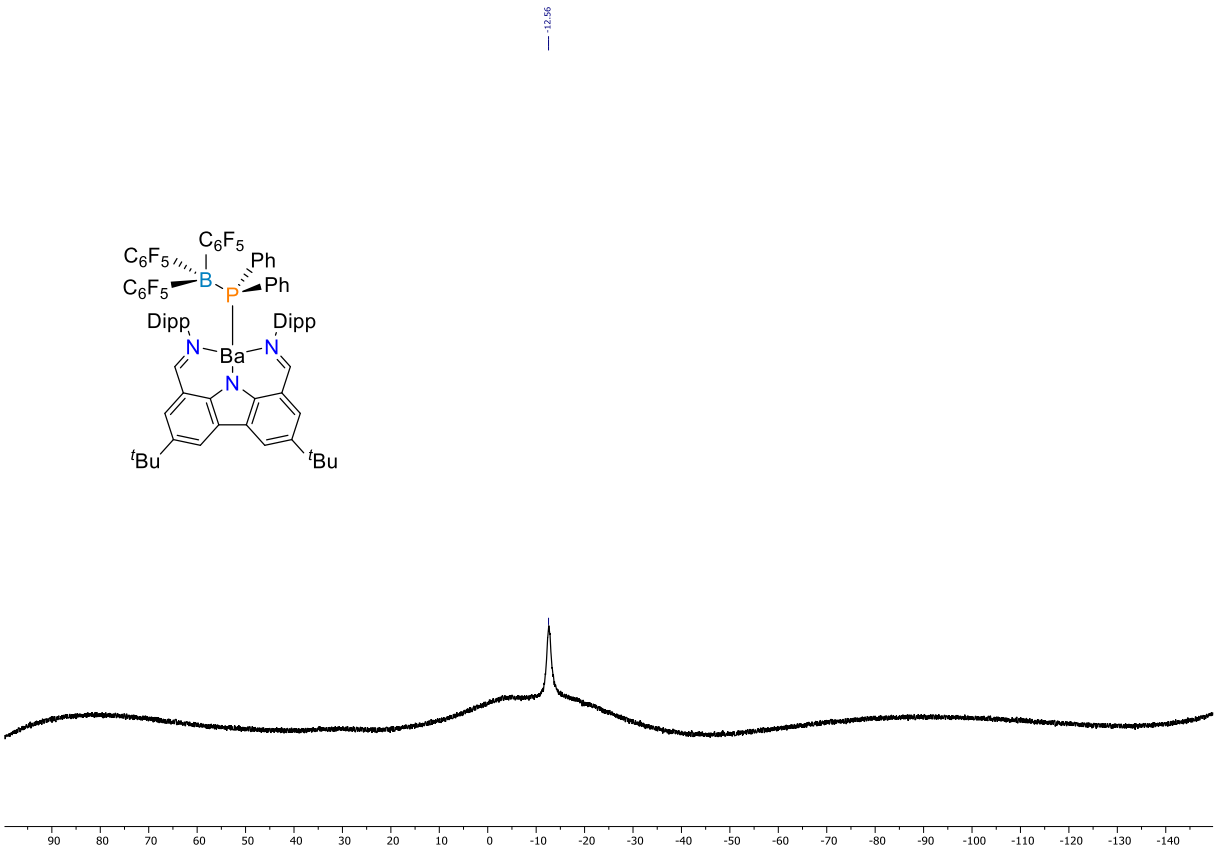

Figure S19. ^{11}B NMR spectrum (128.38 MHz, toluene-d_8, 298 K) of [{Carb}Ba{PPh_2.$B(C_6F_5)_3$}] (**5**).

NMR spectra for [{Carb}Ba{O(B{C_6F_5}$_3$)$(CH_2)_4PPh_2$}.(thf)] (6)

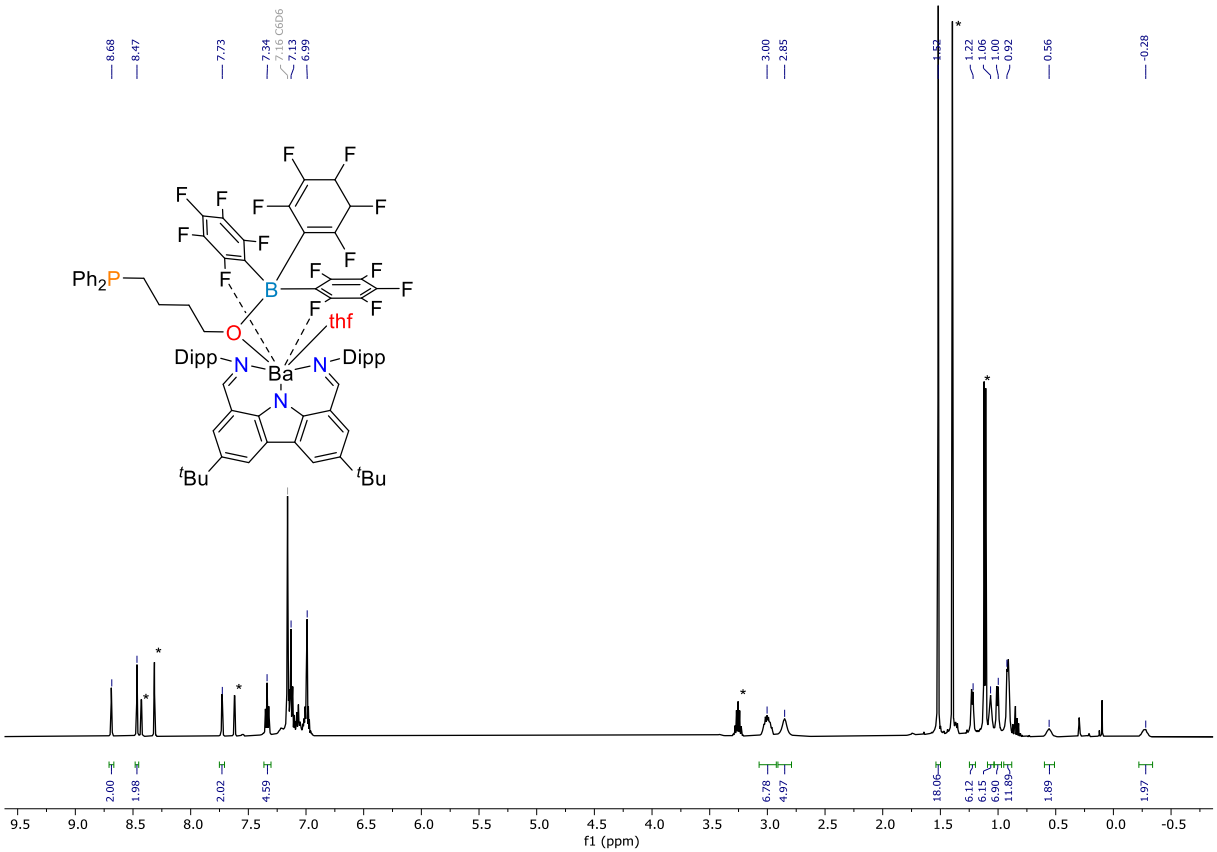

Figure S20. ^{1}H NMR spectrum (500.13 MHz, benzene-d_6, 300 K) of {Carb}Ba{O(B{C_6F_5}$_3$)$(CH_2)_4PPh_2$}.(thf)] (**6**). Additional resonances (*) for hydrolyzed {Carb}H.

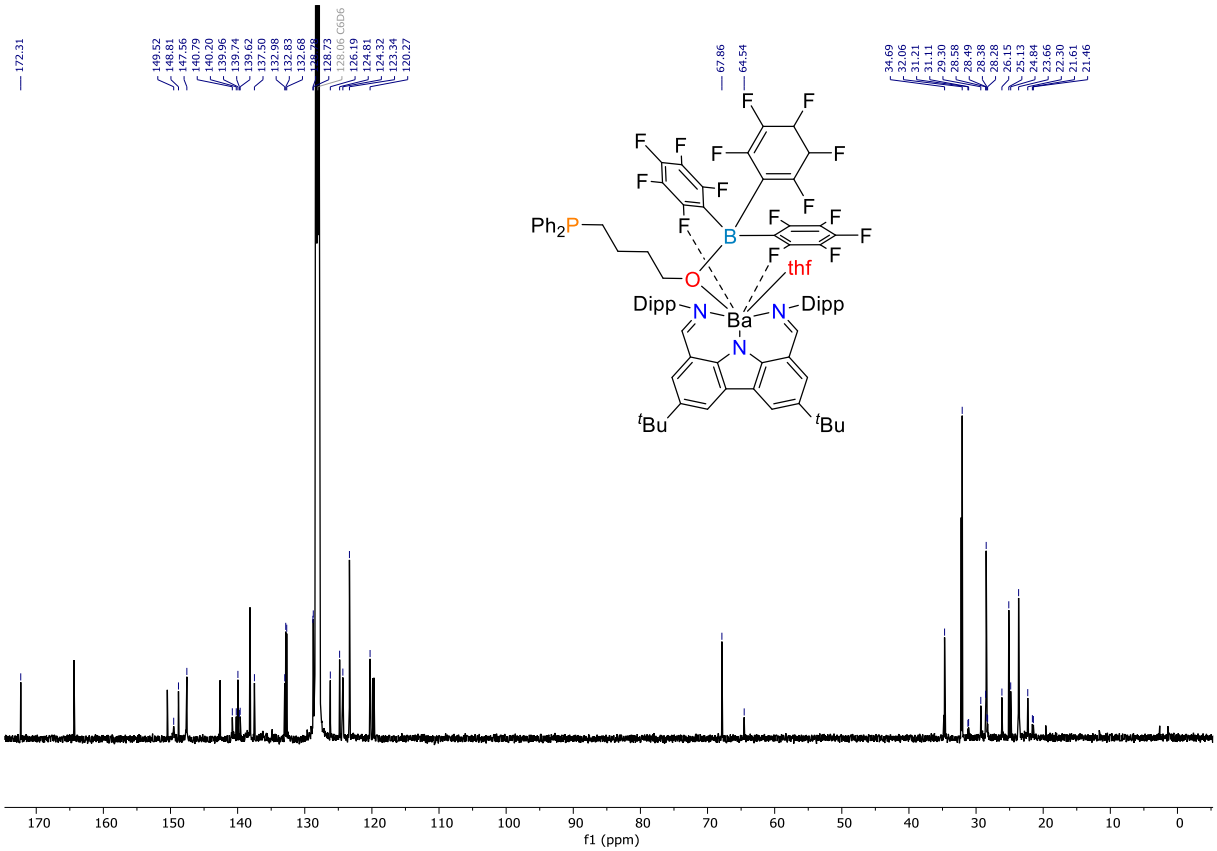

Figure S21. $^{13}C\{^{1}H\}$ NMR spectrum (125.77 MHz, benzene-d_6, 300 K) of {Carb}Ba{O(B{C_6F_5}$_3$)$(CH_2)_4PPh_2$}.(thf)] (**6**). Unpeaked resonances belong to hydrolyzed {Carb}H.

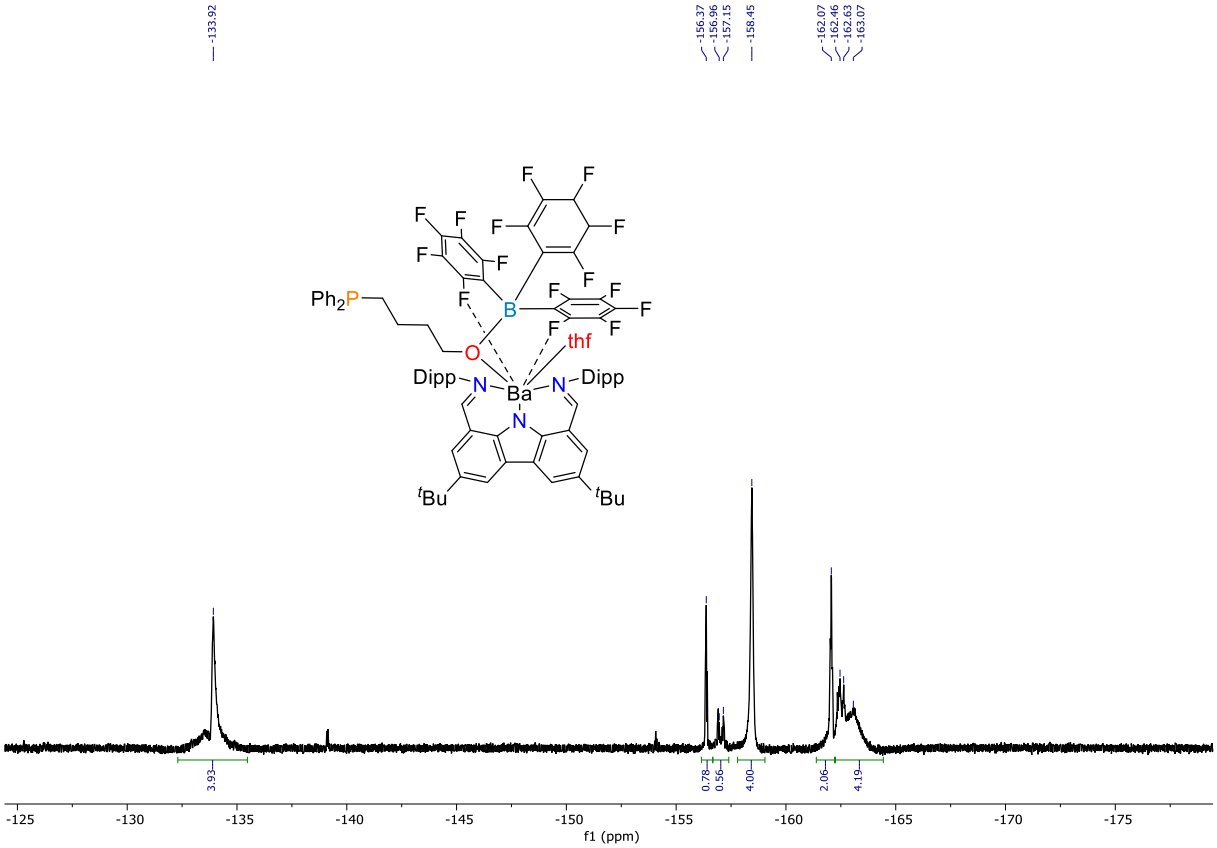

Figure S22. ^{19}F NMR spectrum (470.52 MHz, benzene-d_6, 300 K) of {Carb}Ba{O(B{C_6F_5}$_3$)$(CH_2)_4PPh_2$}.(thf)] (**6**).

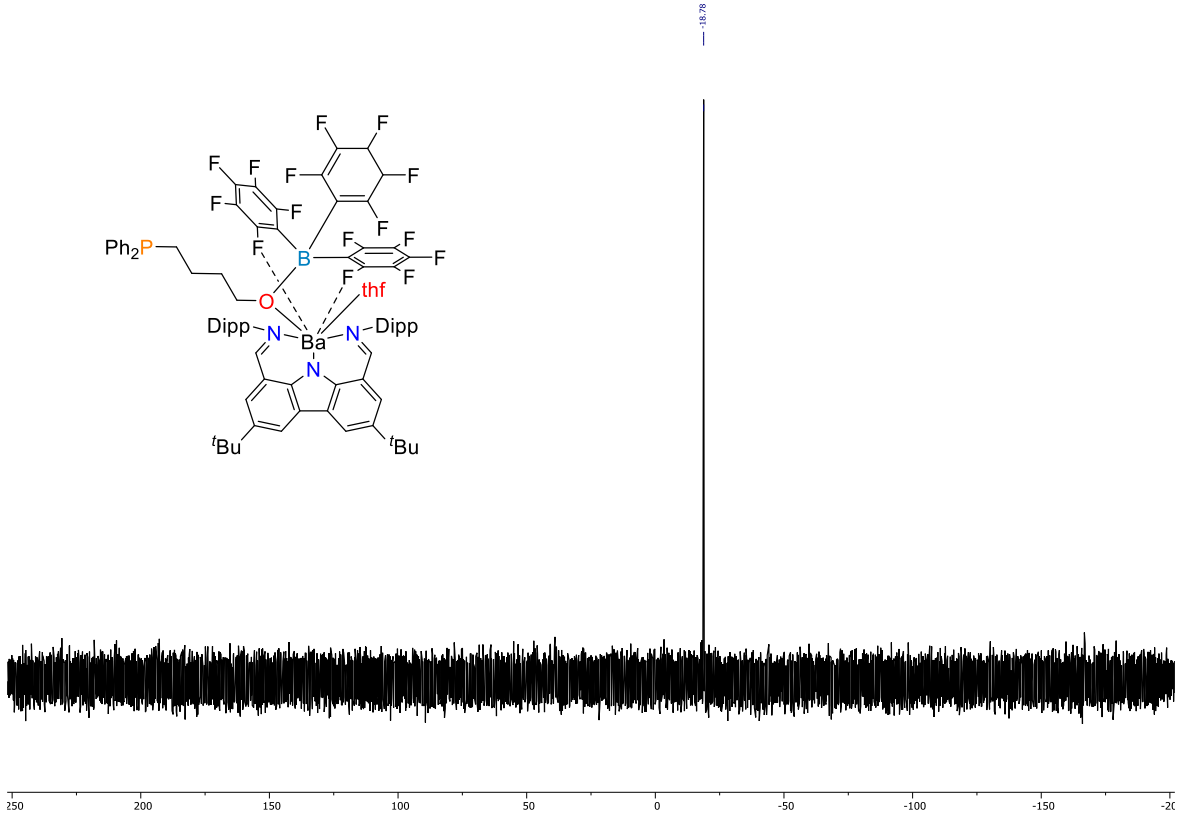

Figure S23. ^{31}P NMR spectrum (161.99 MHz, benzene-d_6, 298 K) of {Carb}Ba{O(B{C_6F_5}$_3$)$(CH_2)_4PPh_2$}.(thf)] (**6**).

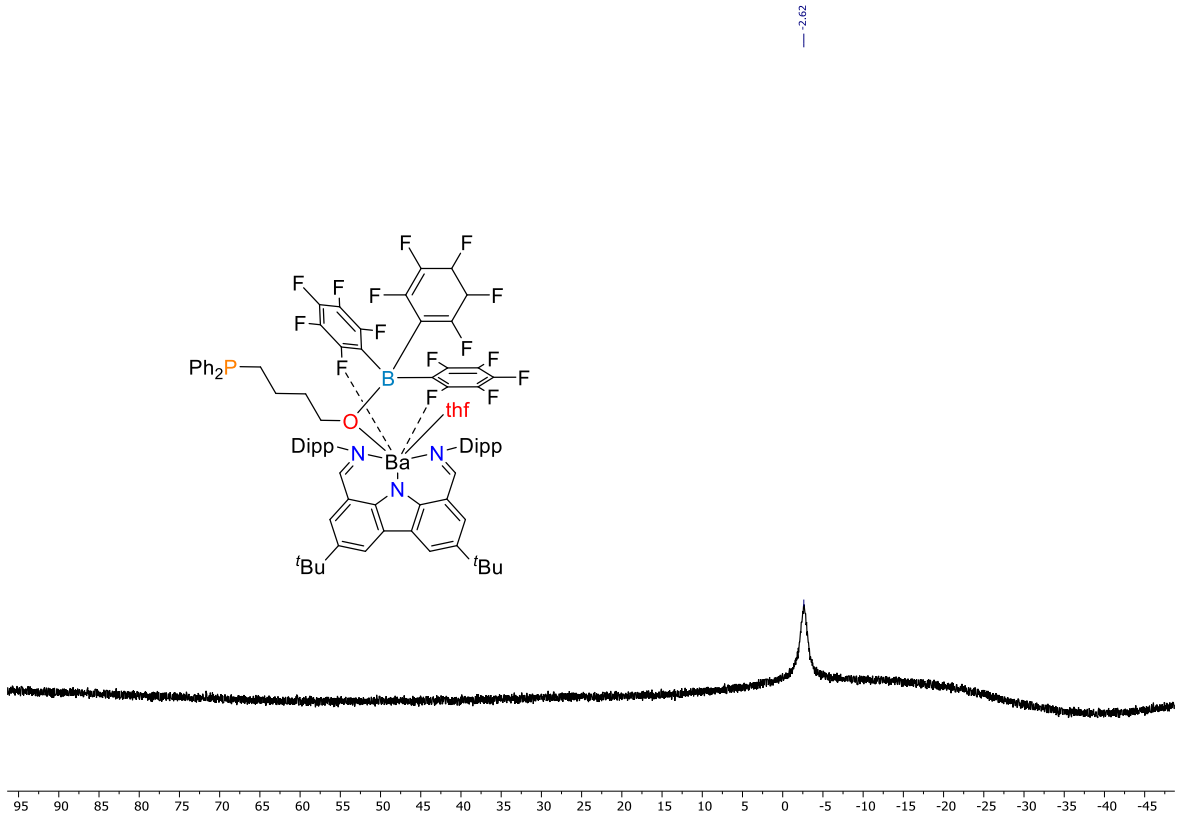

Figure S24. ^{11}B NMR spectrum (128.40 MHz, benzene-d_6, 298 K) of {Carb}Ba{O(B{C_6F_5}$_3$)$(CH_2)_4PPh_2$}.(thf)] (**6**).

NMR spectra for [Ba{O(B{C$_6$F$_5$}$_3$)(CH$_2$)$_4$PPh$_2$}$_2$.(thf)$_{1.5}$] (7)

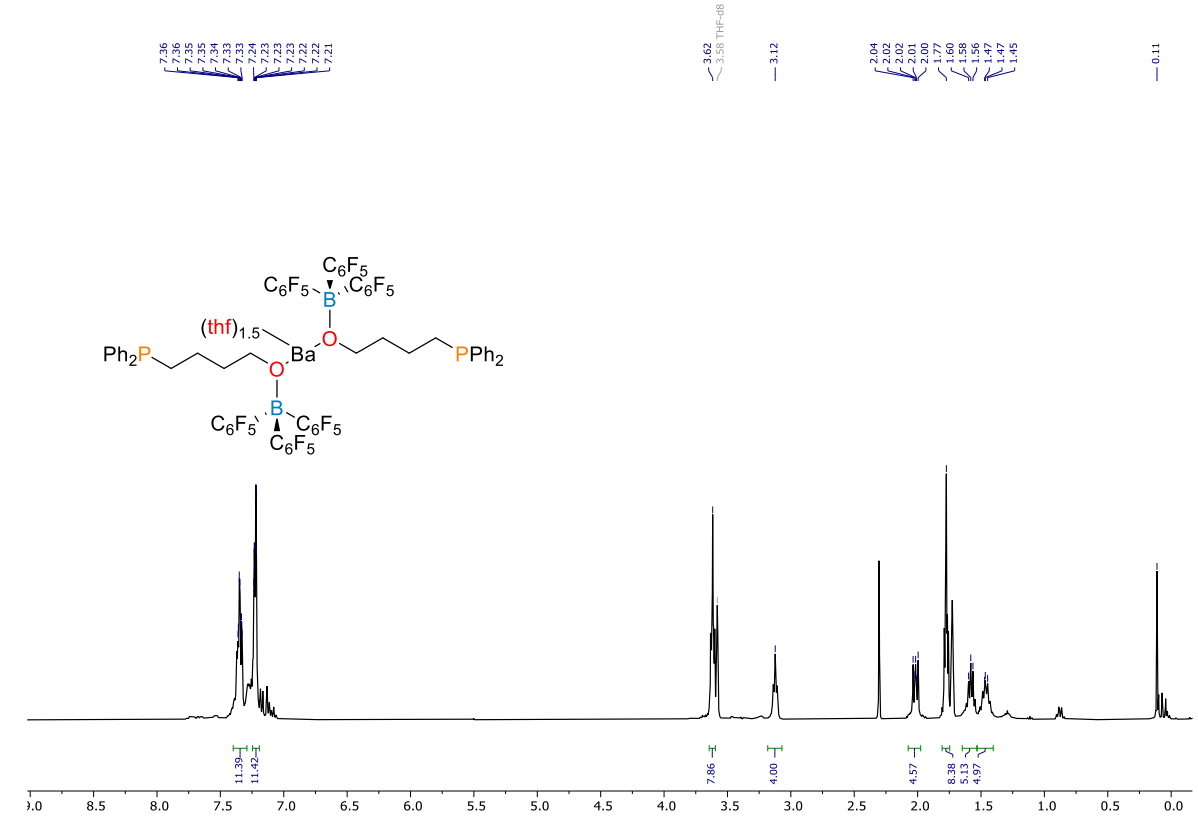

Figure S25. ^{1}H NMR spectrum (400.16 MHz, thf-d_8, 298 K) of [Ba{O(B{C$_6$F$_5$}$_3$)(CH$_2$)$_4$PPh$_2$}$_2$.(thf)$_{1.5}$] (**7**).

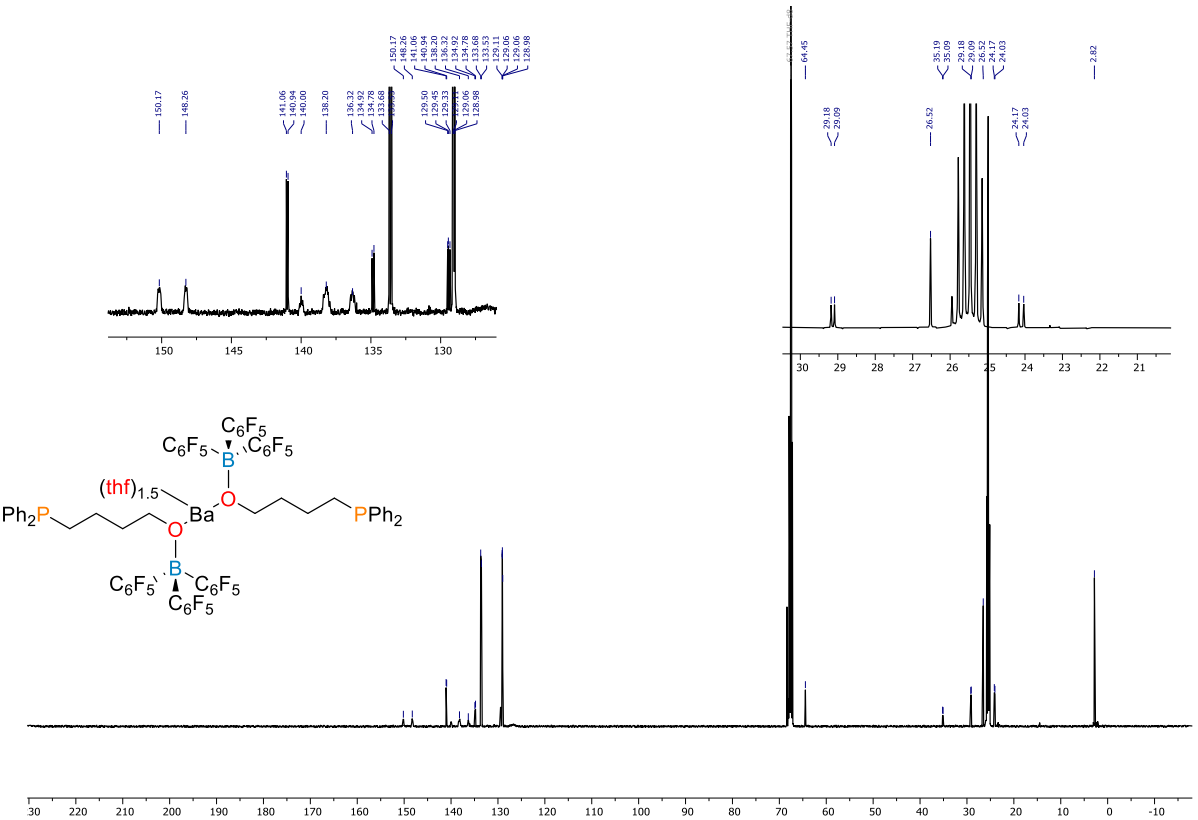

Figure S26. ^{13}C{^{1}H} NMR spectrum (125.77 MHz, thf-d_8, 300 K) of [Ba{O(B{C$_6$F$_5$}$_3$)(CH$_2$)$_4$PPh$_2$}$_2$.(thf)$_{1.5}$] (**7**).

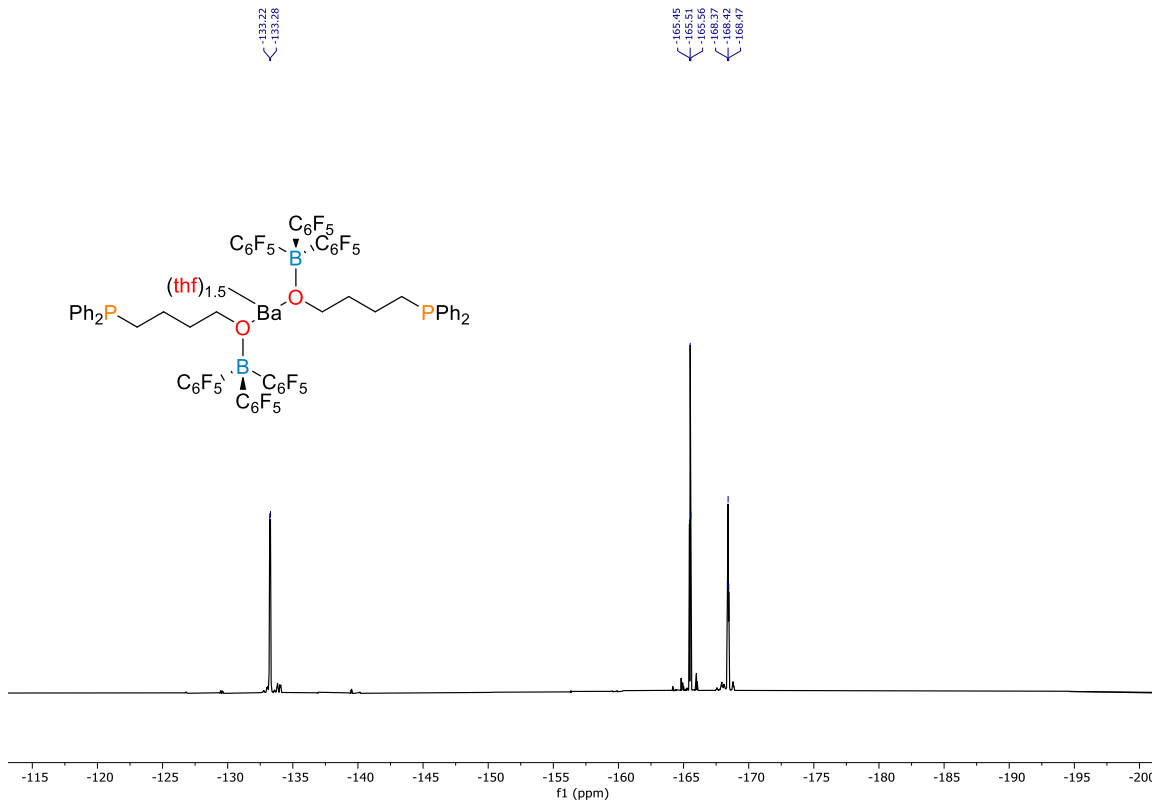

Figure S27. ^{19}F NMR spectrum (376.47 MHz, thf-d_8, 298 K) of [Ba{O(B{C_6F_5}$_3$)$(CH_2)_4PPh_2$}$_2$.$(thf)_{1.5}$] (**7**).

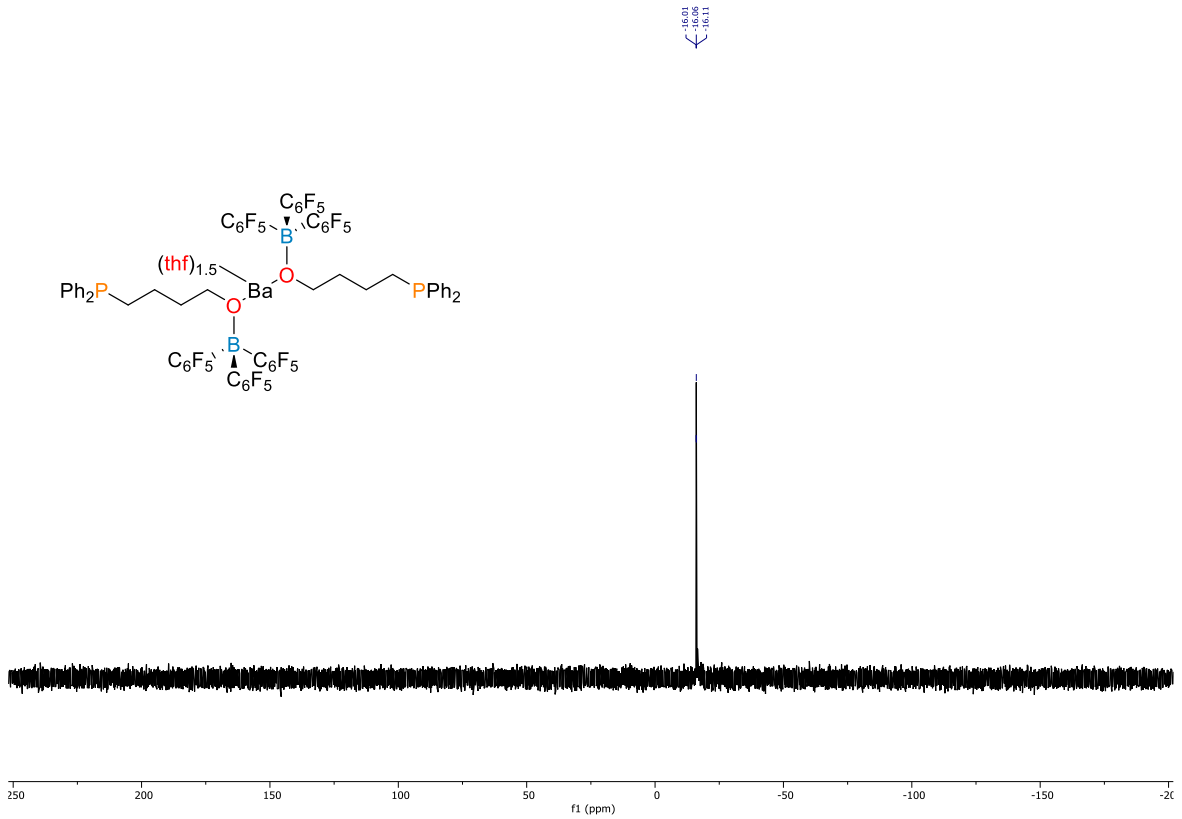

Figure S28. ^{31}P NMR spectrum (161.99 MHz, thf-d_8, 298 K) of [Ba{O(B{C_6F_5}$_3$)$(CH_2)_4PPh_2$}$_2$.$(thf)_{1.5}$] (**7**).

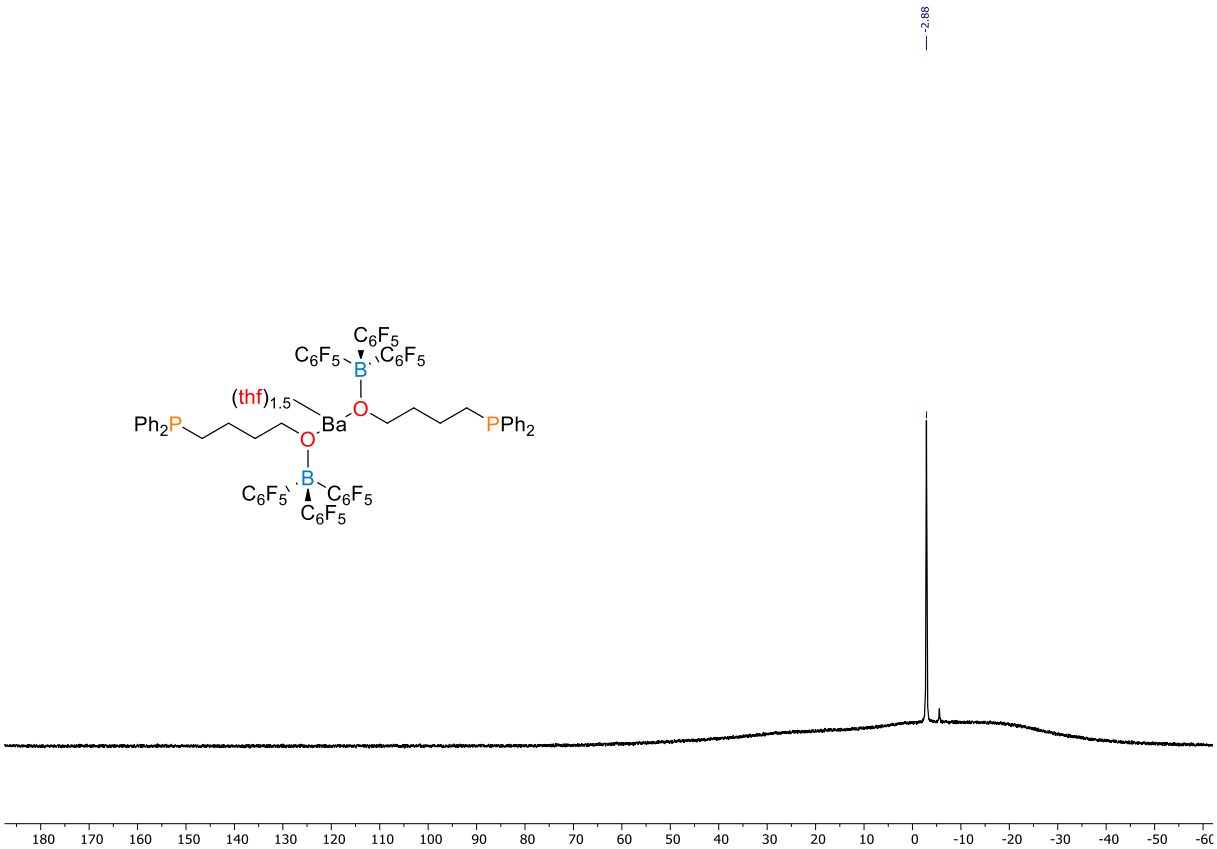

Figure S29. ^{11}B NMR spectrum (128.40 MHz, thf-d_8, 298 K) of [Ba{O(B{C_6F_5}$_3$)$(CH_2)_4PPh_2$}$_2$.$(thf)_{1.5}$] (**7**).

NMR spectra for [Ba{$PPh_2.B(C_6F_5)_3$}$_2$.$(thp)_2$] (8)

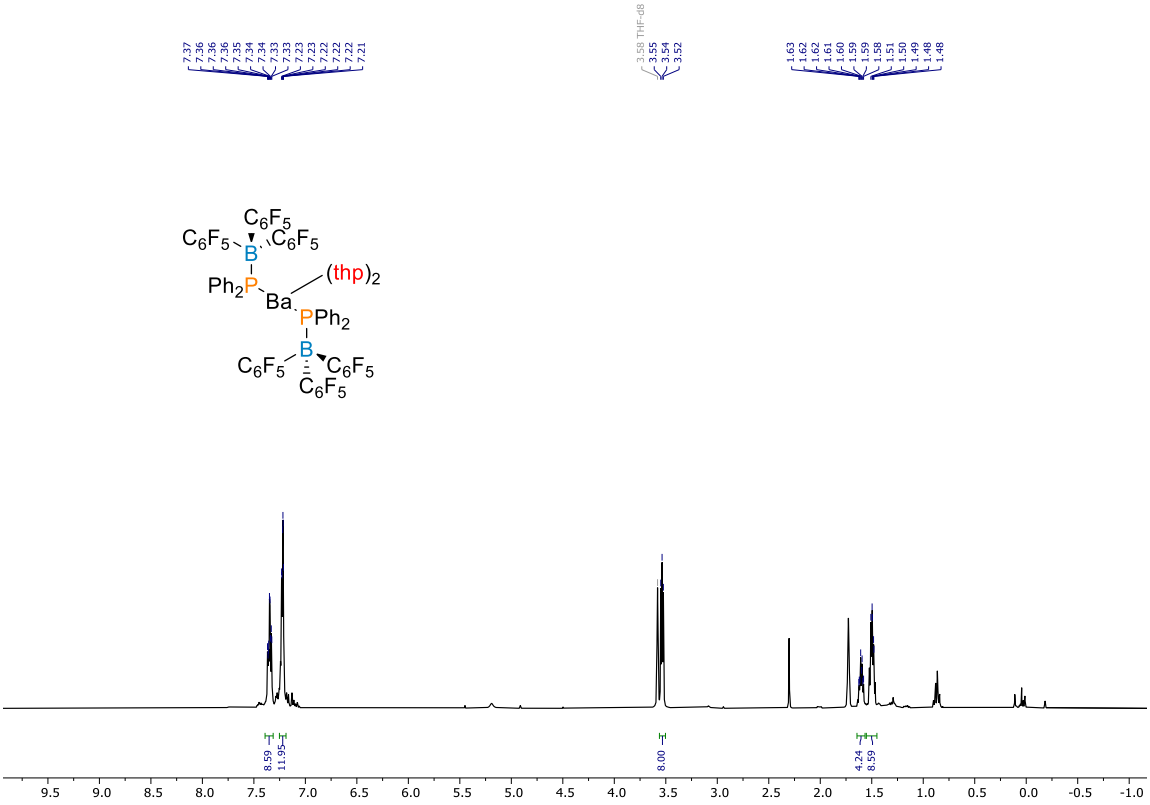

Figure S30. ^{1}H NMR spectrum (400.16 MHz, thf-d_8, 300 K) of [Ba{$PPh_2.B(C_6F_5)_3$}$_2$.$(thp)_2$] (**8**).

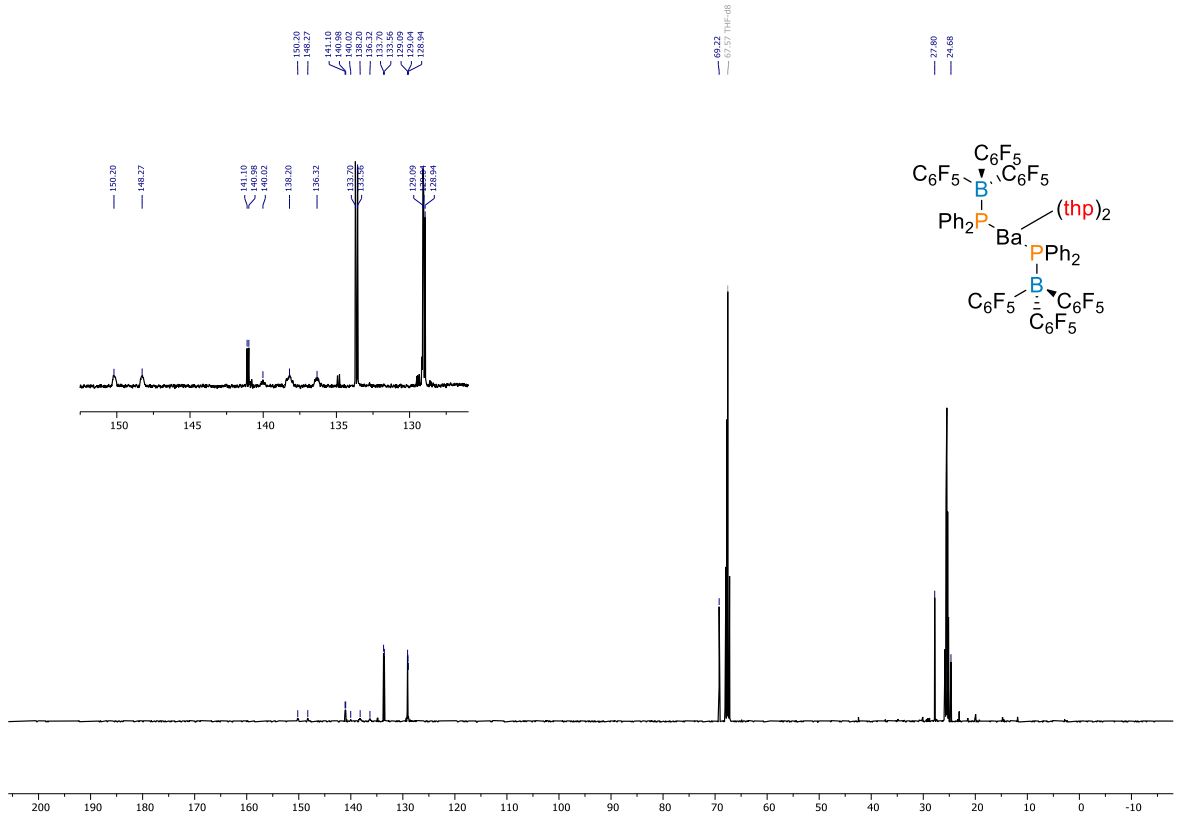

Figure S31. ^{13}C{^{1}H} NMR spectrum (125.77 MHz, thf-d_8, 300 K) of [Ba{$PPh_2.B(C_6F_5)_3$}$_2$.$(thp)_2$] (**8**). **Inset**: The aromatic carbon resonances from 120-160 ppm.

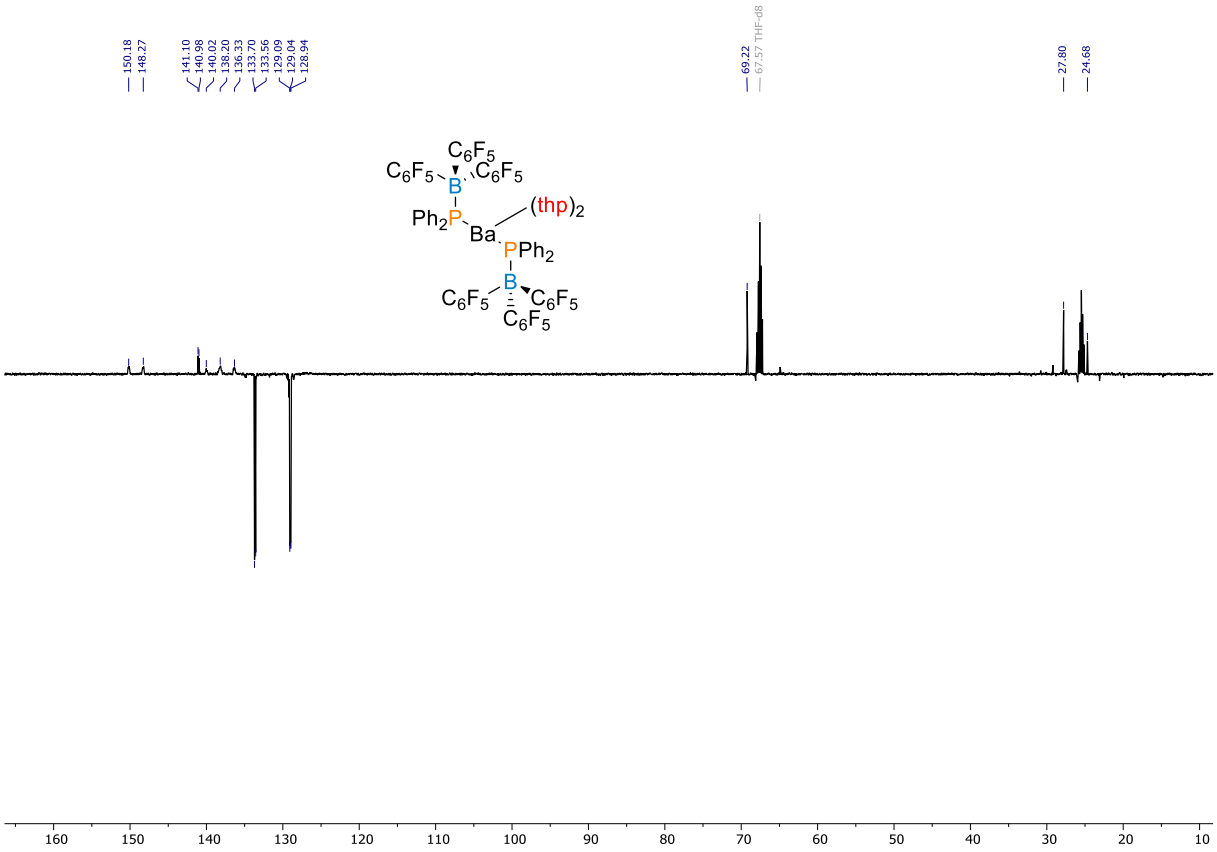

Figure S32. ^{13}C DEPT NMR spectrum (125.77 MHz, thf-d_8, 300 K) of [Ba{PPh_2.B(C_6F_5)$_3$}$_2$.(thp)$_2$] (**8**).

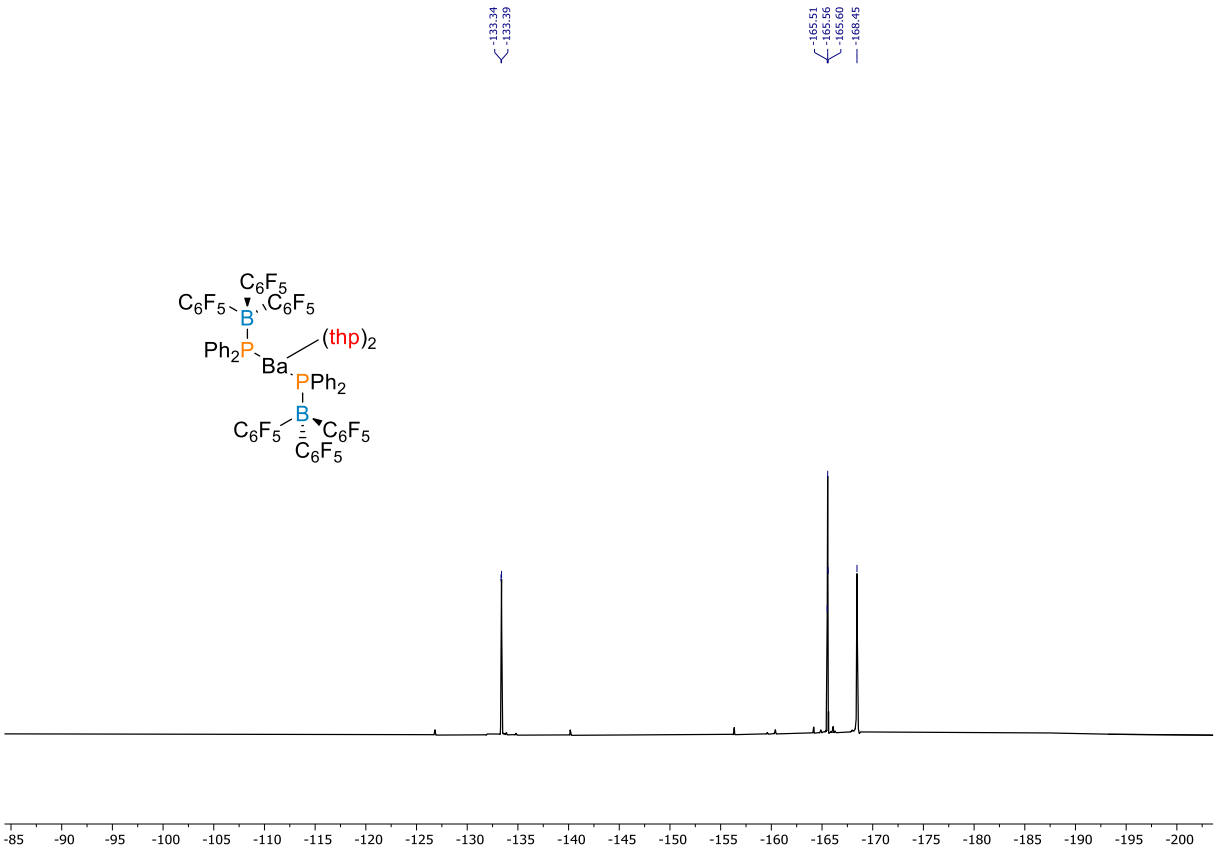

Figure S33. ^{19}F NMR spectrum (470.52 MHz, thf-d_8, 300 K) of [Ba{PPh_2.B(C_6F_5)$_3$}$_2$.(thp)$_2$] (**8**).

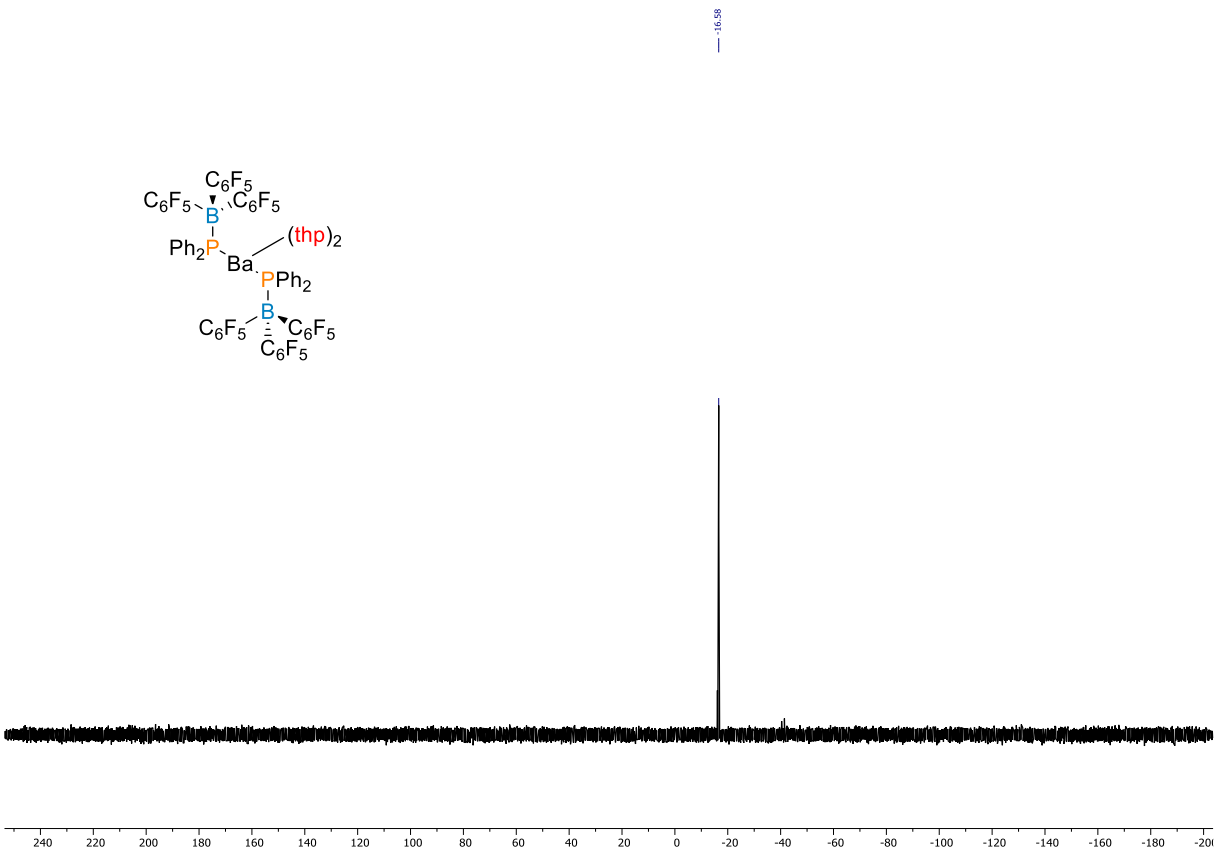

Figure S34. ^{31}P NMR spectrum (202.46 MHz, thf-d_8, 300 K) of [Ba{PPh_2.B(C_6F_5)$_3$}$_2$.(thp)$_2$] (**8**).

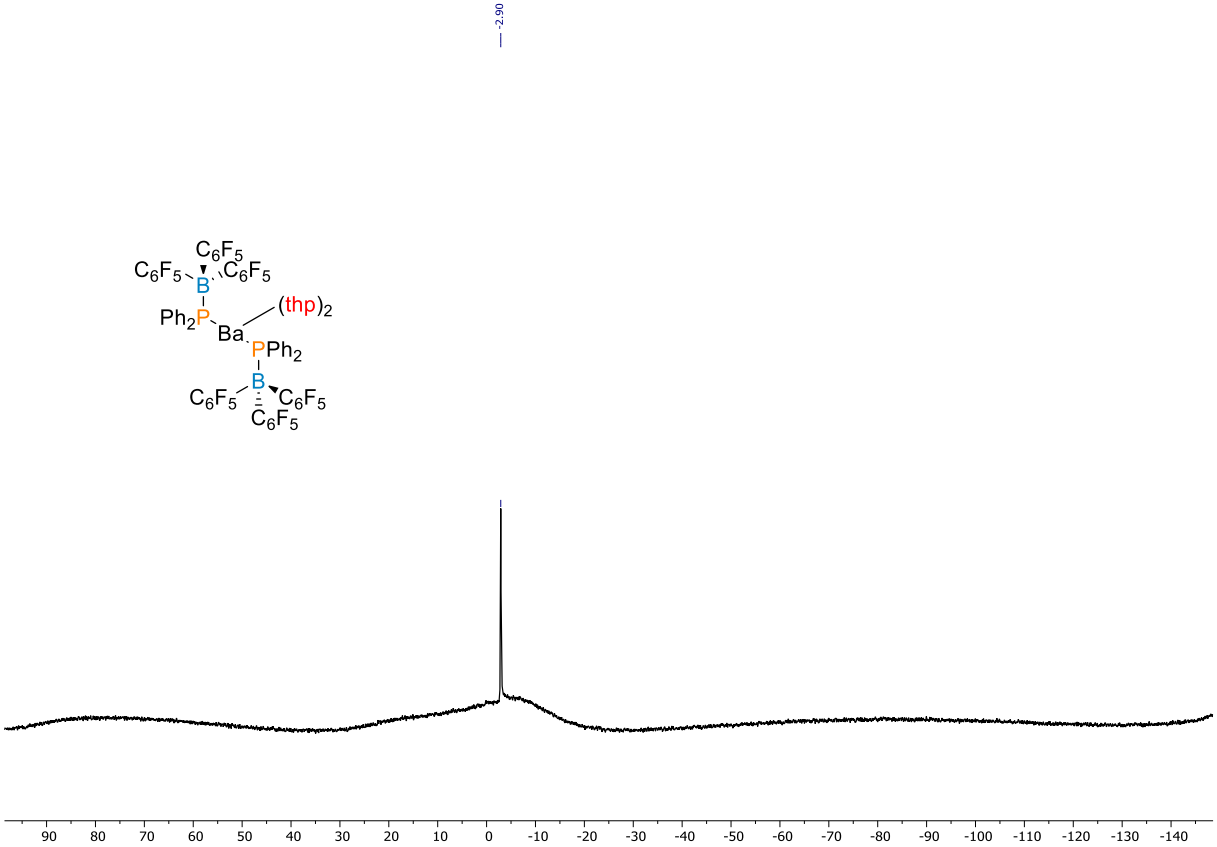

Figure S35. ^{11}B NMR spectrum (160.46 MHz, thf-d_8, 300 K) of [Ba{PPh_2.B(C_6F_5)$_3$}$_2$.(thp)$_2$] (**8**).

X-ray diffraction crystallography details

Compound number	Complex number	Experiment number	CCDC number
[{Carb}Ba(PPh_2).$(thf)_2$]	**1.$(thf)_2$**	PC2040	2314377
[{Carb}Ca{$(H_3B)_2PPh_2$}.(thf)]	**4**	PC051342thf_2	2314378
[{Carb}Ba{$O(B(C_6F_5)_3)(CH_2)_4PPh_2$}.thf]	**6**	PC05150	2314379
[Ba{$PPh_2.B(C_6F_5)_3$}$_2$.$(thp)_2$]	**8**	PC06040fr	2314380

[{Carb}Ba(PPh_2).$(thf)_2$] (1.$(thf)_2$)

($C_{66}H_{85}BaN_3O_2P\cdot 3(C_4H_8O)$); M = 1336.03. D8 VENTURE Bruker AXS diffractometer equipped with a (CMOS) PHOTON 100 detector, Mo-Kα radiation (λ = 0.71073 Å, multilayer monochromator), T = 150(2) K; triclinic P-1 (I.T.#2), a = 13.7946(18), b = 14.2052(16), c = 20.139(2) Å, α = 75.420(4), β = 78.239(5), γ = 70.451(4) °, V = 3568.1(8) $Å^3$. Z = 2, d = 1.244 $g.cm^{-3}$, μ = 0.630 mm^{-1}. The structure was solved by dual-space algorithm using the SHELXT program,[5] and then refined with full-matrix least-squares methods based on F2 (SHELXL).[6] The contribution of the disordered solvents to the calculated structure factors was estimated following the BYPASS algorithm,[7] implemented as the SQUEEZE option in PLATON.[8] A new data set, free of solvent contribution, was then used in the final refinement. All non-hydrogen atoms were refined with anisotropic atomic displacement parameters. H atoms were finally included in their calculated positions and treated as riding on their parent atom with constrained thermal parameters. A final refinement on F^2 with 15909 unique intensities and 708 parameters converged at ωR(F^2) = 0.2756 (R_F = 0.1224) for 12302 observed reflections with I > 2σ(I).

[{Carb}Ca{$(H_3B)_2PPh_2$}.(thf)] (**4**)

($C_{62}H_{82}B_2CaN_3OP$); M = 977.97. A suitable crystal for X-ray diffraction single crystal experiment (yellow prism, dimensions = 0.330 x 0.270 x 0.130 mm) was selected and mounted with a cryoloop on the goniometer head of a APEXII Kappa-CCD diffractometer equipped with a CCD plate detector , using Mo-Kα radiation (λ = 0.71073 Å, graphite monochromator) at T = 150(2) K. Crystal structure has been described in monoclinic symmetry and P 2_1 (I.T.#4) acentric space group. Cell parameters have been founded as follows: a = 13.0239(10), b = 12.5202(9), c = 18.2775(12) Å, β = 99.281(3) °, V = 2941.3(4) $Å^3$. Number of formula unit Z is equal to 2 and calculated density *d* and absorption coefficient μ values are 1.104 $g.cm^{-3}$ and 0.175 mm^{-1} respectively. The structure was solved by dual-space algorithm using the SHELXT program,[5] and then refined with full-matrix least-squares methods based on F^2 (SHELXL program[6]). All non-hydrogen atoms were refined with anisotropic atomic displacement parameters. Except hydrogen atoms linked to boron atoms that were introduced in the structural model through Fourier difference maps analysis, H atoms were finally included in their calculated positions and treated as riding on their parent atom with constrained thermal parameters. A final refinement on F^2

with 10613 unique intensities and 644 parameters converged at ωR(F^2) = 0.0933 (R_F = 0.0412) for 9566 observed reflections with (I > 2σ).

[{Carb}Ba{O(B(C_6F_5)$_3$)$CH_2CH_2CH_2CH_2PPh_2$}.thf] (6)

$C_{84}H_{84}BBaF_{15}N_3O_2P \cdot C_6H_{14}$); M = 1717.87. A suitable crystal for X-ray diffraction single crystal experiment (yellow prism, dimensions = 0.300 x 0.180 x 0.150 mm) was selected and mounted with a cryoloop on the goniometer head of a APEXII Kappa-CCD diffractometer equipped with a (CMOS) PHOTON 100 detector, using MoKα radiation (λ = 0.71073 Å, multilayer monochromator) at T = 150(2) K. Crystal structure has been described in triclinic symmetry and P -1 (I.T.#2) centric space group. Cell parameters have been refined as follows: a = 15.537(2), b = 16.193(2), c = 18.240(2) Å, α = 80.945(4), β = 67.840(4), γ = 88.782(4) °, V = 4193.4(9) Å^3 . Number of formula unit Z is equal to 2 and calculated density *d* and absorption coefficient μ values are 1.361 g.cm^{-3} and 0.575 mm^{-1} respectively. The structure was solved by dual-space algorithm using the SHELXT program,[5] and then refined with full-matrix least-squares methods based on F^2 (SHELXL program[6]). The contribution of the disordered solvents to the calculated structure factors was estimated following the BYPASS algorithm,[7] implemented as the SQUEEZE option in PLATON.[8] A new data set, free of solvent contribution, was then used in the final refinement. All non-Hydrogen atoms were refined with anisotropic atomic displacement parameters. H atoms were finally included in their calculated positions and treated as riding on their parent atom with constrained thermal parameters. A final refinement on F^2 with 19189 unique intensities and 965 parameters converged at ωR(F^2) = 0.1207 (R_F = 0.0479) for 14909 observed reflections with (I > 2σ).

[Ba{PPh_2.B(C_6F_5)$_3$}$_2$.(thp)$_2$] (8)

($C_{70}H_{40}B_2BaF_{30}O_2P_2 \cdot C_7H_8$); M = 1796.05. A suitable crystal for X-ray diffraction single crystal experiment (colourless prism, dimensions = 0.520 x 0.330 x 0.230 mm) was selected and mounted with a cryoloop on the goniometer head of a APEXII Kappa-CCD (Bruker-AXS) diffractometer equipped with a CCD plate detector, using Mo-Kα radiation (λ = 0.71073 Å, graphite monochromator) at T = 150(2) K. Crystal structure has been described in monoclinic symmetry and C 2/c (I.T.#15) centric space group. Cell parameters have been refined as follows: a = 49.3823(17), b = 14.4529(5), c = 21.5081(8) Å, β = 107.6180(10) °, V = 14630.7(9) Å^3 . Number of formula unit Z is equal to 8 and calculated density *d* and absorption coefficient μ values are 1.631 g.cm^{-3} and 0.711 mm^{-1} respectively. Crystal structure was solved by dual-space algorithm using SHELXT program,[5] and then refined with full-matrix least-squares methods based on F^2 (SHELXL program[6]). All non-Hydrogen atoms were refined with anisotropic atomic displacement parameters. H atoms were finally included in their calculated positions and treated as riding on their parent atom with constrained thermal parameters. A final refinement on F^2 with 16431 unique intensities and 964 parameters converged at ωR(F^2) = 0.1138 (R_F = 0.0429) for 12168 observed reflections with (I > 2σ).

DFT calculations.

Density functional theory (DFT) calculations were performed using the Amsterdam Density Functional ADF2019 code.[9] Scalar relativistic effects were taken into account via the Zeroth Order Regular Approximation (ZORA).[10] A triple-zeta basis set augmented with two polarisation function (STO-TZ2P)[11] was used together with the PBE0 functional[12-13] and Grimme's empirical DFT-D3(BJ) corrections[14] for geometry optimisation and analytical vibrational frequency computations. Natural atomic orbital (NAO) populations and Wiberg bond indices were computed with the NBO6.0 program.[15] Interaction energy between fragments were computed according to the Morokuma-Ziegler energy decomposition analysis (EDA) formalism[16-18] implemented in the ADF2019 program. The QTAIM analysis[19-20] was performed as implemented in the ADF2019 suite.[21-22] In addition, xyz files for all optimized structures are provided in attachment.

Table S1. Relevant DFT-computed data for **6**

Bond distances / Å [WBIs[b]]	**Ba-$N_{carb.}$**	**Ba-$N_{imin.}$[a]**	**Ba-$O_{alk.}$**	**Ba-O_{THF}**	**Ba…F73**	**Ba…F95**
	2.654 [0.050]	2.769 [0.028]	2.740 [0.026]	2.769 [0.020]	2.990 [0.011]	2.813 [0.012]
Atomic charges	**Ba**	**N_{carb}**	**$N_{imin.}$[a]**	**O_{alk}**	**O_{THF}**	**F [a,c]**
Natural	+1.82	-0.68	-0.58	-0.79	-0.60	-0.36
QTAIM	+1.68	-1.12	-1.21	-1.33	-1.12	-0.69
QTAIM descriptors of the Ba···F bonds / a.u. [a,d]	δ	ρ	$\nabla^2\rho$	**H**	**V**	**$\lvert V \rvert$/G**
	0.077	0.015	0.074	0.003	-0.050	0.77

[a] Averaged values. [b] Wiberg bond indices. [c] Ba-connected fluorines only. [d] ρ, $\nabla^2\rho$, H, V and G are the electron density, Laplacian of ρ density, energy density, potential energy density and kinetic energy density values at the bcp, respectively

Table S2. Relevant DFT-computed data for **8**

Bond distances [a] / Å [WBIs] [a,b]	**Ba-P**	**Ba-O**	**Ba-F**	**P-B**		
	3.205 [0.057]	2.685 [0.026]	2.854 [0.011]	2.057 [0.856]		
X-ray distances [a]	3.279(3)	2.640(2)	2.856(3)	2.060(4)		
Atomic charges	**Ba**	**P [a]**	**O [a]**	**F [a]**	**B**	
Natural	+1.82	+0.32	-0.62	-0.37	+0.16	
QTAIM	+1.66	+0.73	-1.13	-0.70	+1.58	
QTAIM descriptors of the:	δ	ρ	$\nabla^2\rho$	**H**	**V**	**$\lvert V \rvert$/G**
Ba–P bonds / a.u. [a,c]	0.220	0.028	0.047	-0.004	-0.018	1.211
Ba···F bonds / a.u. [a,c]	0.085	0.016	0.082	0.004	-0.013	0.77

[a] Averaged values. [b] Wiberg bond indices. [c] Ba-connected fluorines only. [d] ρ, $\nabla^2\rho$, H, V and G are the electron density, Laplacian of ρ density, energy density, potential energy density and kinetic energy density values at the bcp, respectively

References

1 Chapple, P. M.; Kahlal, S.; Cartron, J.; Roisnel, T.; Dorcet, V.; Cordier, M.; Saillard, J.-Y.; Carpentier, J.-F.; Sarazin, Y. Bis(imino)carbazolate: a master key for barium chemistry. *Angew. Chem. Int. Ed.* **2020**, *59*, 9120-9126.

2 Lancaster, S. J.; Mountford, A. J.; Hughes, D. L.; Schormann, M.; Bochmann, M. Ansa-metallocenes with B-N and B-P linkages: the importance of N-H···F-C hydrogen bonding in pentafluorophenyl boron compounds. *J. Organomet. Chem.* **2003**, *680*, 193-205.

3 Boncella, J. M.; Coston, C. J.; Cammack, J. K. The synthesis of bis(hexamethyldisilylamido) barium(II). *Polyhedron* **1991**, *10*, 769-770.

4 Bourumeau, K.; Gaumont, A. C.; Denis, J. M. P-H bond activation of primary phosphine-boranes: Access to alpha-hydroxy and alpha, alpha′-dihydroxyphosphine-borane adducts by uncatalyzed hydrophosphination of carbonyl derivatives. *J. Organomet. Chem.* **1997**, *529*, 205-213.

5 Sheldrick, G. M., SHELXT - Integrated space-group and crystal-structure determination, *Acta Cryst.*, **2015**, A71, 3.

6 Sheldrick, G. M., Crystal structure refinement with SHELXL, *Acta Cryst.*, **2015**, C71, 3.

7 Sluis, P. V. D., Spek, A. L., BYPASS: an effective method for the refinement of crystal structures containing disordered solvent regions *Acta Cryst.*, **1990**, A46, 194.

8 Spek, A. L., Single-crystal structure validation with the program PLATON *J. Appl. Cryst.*, **2003**, 36, 7.

9 (*a*) G. te Velde, F. M. Bickelhaupt, S. J. A. van Gisbergen, C. F. Guerra, E. J. Baerends, G. J. Snijders and Ziegler, T. *J. Comput. Chem.*, 2001, **22**, 931-967; (*b*) ADF 2019.3, SCM, Theoretical Chemistry, Vrije Universiteit, Amsterdam, The Netherlands, http://www.scm.com.

10 E. van Lenthe, E. J. Baerends and J. G. Snijders, *J. Chem. Phys.*, 1994, **101**, 9783-9792.

11 E. V. Lenthe and E. J. Baerends, *J. Comput. Chem.*, 2003, **24**, 1142-1156.

12 J. P. Perdew, K. Burke and M. Ernzerhof, *Phys. Rev. Lett.*, 1996, **77**, 3865-3868.

13 C. Adamo and V. Barone, *J. Chem. Phys.*, 1999, **110**, 6158-6170.

14 S. Grimme, *J. Comput. Chem.*, 2006, **27**, 1787-1799.

15 E. D. Glendening, J. K. Badenhoop, A. E. Reed, J. E. Carpenter, J. A. Bohmann, C. M. Morales and F. Weinhold, NBO 6.0, University of Wisconsin (Madison, WI, 2001, http://nbo6.chem.wisc.edu).

16 K. Morokuma, *J. Chem. Phys.*, 1971, **55**, 1236-1244.

17 T. Ziegler and A. Rauk, *Inorg. Chem.*, 1979, **18**, 1558-1565.

18 F. M. Bickelhaupt and E. J. Baerends, Kohn-Sham Density Functional Theory: predicting and understanding chemistry. *Rev. Comput. Chem.*; Eds. K. B. Lipkowitz and D. B. Boyd; Wiley, New York 2000, **15**, 1-86.

19 R. F. W. Bader, Atoms in molecules - A quantum theory; Oxford University Press: Oxford, England, 1990.

20 P. L. A. Popelier, in The chemical bond, Eds. G. Frenking and S. Shaik, Wiley-VCH, 2014, **1**, 271-308.

21 J. I. Rodríguez, R. F. W. Bader, P. W. Ayers, C. Michel, A. W. Götz and C. Bo, *Chem. Phys. Lett.*, 2009, **472**, 149-152.

22 J. I. Rodríguez, *J. Comput. Chem.*, **2013**, *34*, 681-686.